Chapter 2

Literature Review

Living bone is an electrically active tissue, therefore, the need for the prosthetic implant materials having inherent / induced mechano-electrical characteristics, mimicking with that of bone, are highly desirable. These mechano-electrically active prosthetic implant materials are a new class of biomaterial. The present chapter is divided in two parts, the first part covers the necessity to develop an electrical equivalent of a typical living cell to understand the effect of external E-field on cells and tissues and second part discusses the electroactive property of hydroxyapatite (HA), which is structurally, chemically and compositionally similar to the bone apatite. Also, the presence of ferroelectricity in HA has been discussed from the view point of consideration of the occurrence of polar phase. Further, the surface charge induced accelerated cellular growth and proliferation on HA has been elaborately discussed in vitro and in vivo. In addition, bone is also a classical example of functionally graded material (FGM), therefore, this chapter also discusses the need to develop the FGM and its advantages over conventional implant materials.

2.1. Bone as an electrically active tissue

2.1.1. Bone biology

Living bone is a natural composite material which is comprised of inorganic mineral phase (hydroxyapatite), organic phase (collagen), bone cells (osteogenic, osteoclasts, osteoblasts, and osteocytes) and fluids (water, extracellular matrix).[1,2] The inorganic hydroxyapatite phase is highly non-stoichiometric, defective as well as contain cations (Ca^{2+}) and complex anions (PO_4^{3-}, CO_3^{2-}) groups along with small impurity ions such as Mg^{2+}, Fe^{2+}, F^-, Cl^-, Na^+ and K^+.[2] The biological mineral apatite have different composition and crystalline nature from synthetic as well as naturally occurring apatite which overall results in different mechanical properties.[2]

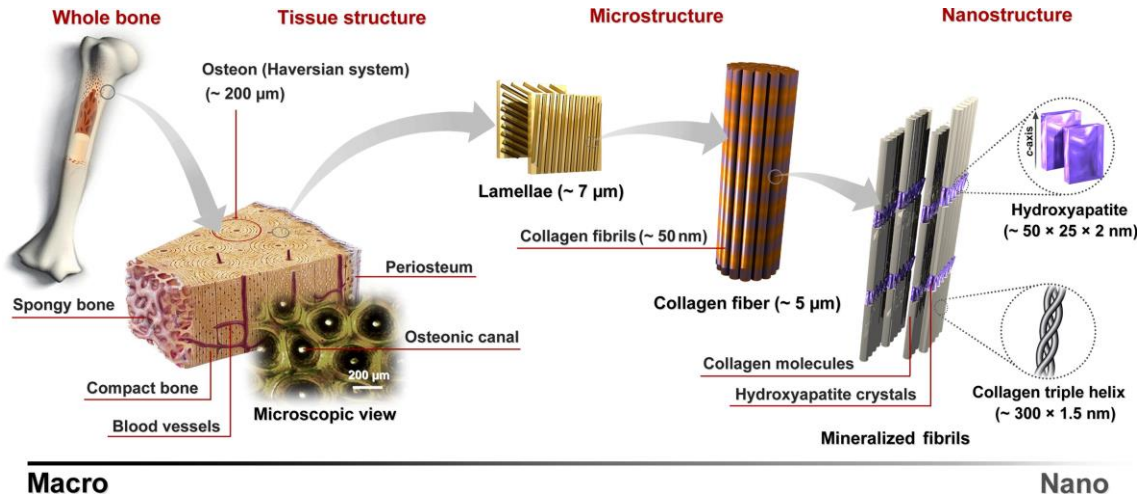

Fig. 2.1: Compact bone represented in a hierarchical structure from micro to nanometer scale.[3] (Reproduced with permission from Elsevier)

Organic phase collagens are protein fibrils. Structurally, these collagen protein fiber are triple helix with a diameter of 1.5 nm and a length of 300 nm, each attached through mineral hydroxyapatite plates with a thickness of ~ 1 nm and a diameter of 70-100 nm [Fig.2.1].[4] The group of collagen fibrils forms lamella. The group of lamella i.e., lamellae (4 to 20) concentrically surrounds the central canal system (Harvesian canal), which facilitates nutrients supply, growth and provides healing of fractures.[2] This system runs parallel to the bone axis. [Fig. 2.2]. Lamellae consist of pores and within these pores osteocytes are present.[2] Together this structural arrangement is called an osteon which forms the basic building blocks of bone. Remodelling of the bone is continuously controlled by osteocytes.[2] In addition, they also play a crucial role in the piezoelectricity of the bone.[2] Bone consists of 60% (by weight) mineral apatite phase and 20 % collagen part and fluids.[2]

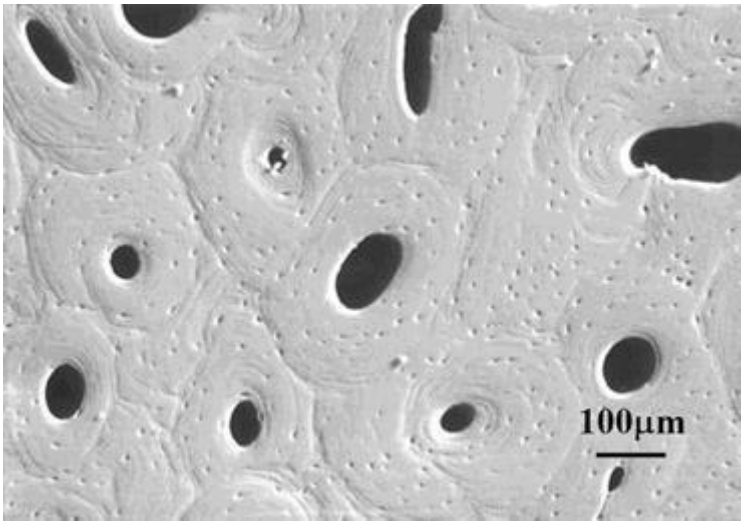

Fig. 2.2: Scanning electron microscopic image of the cross-section of a compact bone depicting the Harvesian systems.[2] (Reproduced with permission from Springer Nature)

Mineral phase in the bone maintains calcium homeostasis resulting in strength as well as stiffness.[1,5] Inorganic/mineral phase is resorbed by osteoclasts.[2] Collagen, on the other hand, provides flexibility as well as tensile strength.[6,7] Collagen has several types (type I, type III, type V, type XII), of which, type I is majorly present in the bone while others are present in small amounts.[2] Osteoblasts synthesize osteoid which contains type I collagen.[2] Living bone is in a state of constant remodelling which is mediated through mechanical loading as well as hormonal responses generated through the variation of calcium and phosphate.[8,9,10] According to Wolff's law, bone structurally adapts, remodels, as well as develops strength depending on the applied mechanical stress/loading.[11,12] When there is no external loading/stress, the bone becomes porous and reduces its mass.[2]

2.1.2. Bone bioelectricity

It is widely known that the living organisms generate endogenous currents because of the presence of the various inorganic ions and their gradients.[13] These endogenous currents guide various functionalities at cellular level such as cell migration, tissue growth as well as wound healing.[14,15] Besides, these endogenous currents also contribute to fetal development.[16]

Therefore, the role of the external electric field becomes crucial to alter the cellular as well as tissue functionalities.[16,17] Living bone is a highly organized anisotropic tissue which remodels and heals through coordinated coupled dynamic electrical processes.[13,18,19] It is recognized as a piezoelectric material.[20] Piezoelectricity was first observed in 1880 in the crystals of Rochelle salt (sodium potassium tartrate), quartz and tourmaline by Jacques and Pierre Curie.[21] It is the property in which mechanical stress creates a certain potential difference or vice versa. From the crystallographic point of view, it can be understood as the compressive or the tensile force which produces the electrical potential difference across the opposite faces of the crystal or vice versa.[2] Considering an ionically bonded substance which is crystalline as well as having ions arranged in its unit cell either symmetrically or asymmetrically. If this arrangement of ions in the individual unit cell is asymmetrical, then an electric dipole would be generated upon external stimulation, which can be temperature, electric field or electromagnetic field, etc. Therefore, when the dipole is mechanically strained, the displacement of positive and negative ions produces a net polarization effect. On the other hand, if electric field is applied, dipoles would get aligned along the field, resulting in the strain effect in the material at the macroscopic level. Overall, it can be suggested that the piezoelectric materials have some form of asymmetry in their lattice. The bending piezoelectricity was first discovered by Yasuda (1953) in long bones.[22] The property was subsequently utilized to heal bone fractures as well as facilitate in its growth through mechanical and electrical stimulation. Further, in 1957, Fukada and Yasuda observed direct as well inverse piezoelectricity in bone in response to shear force.[20] Thereafter, in 1964, shear and tensile piezoelectricity were observed in collagen (tendons) as well as in bones.[23] Overall, it was concluded that living bone is a true piezoelectric material. In 1966, pyroelectricity was discovered in bones by Lang.[24,25] Later on, streaming potentials was recognized in wet bones.[26] It has been suggested that the electro-mechanical transduction of

bones can be described in terms of piezoelectricity as well as streaming potential. In addition, bone is reported to be ferroelectric.[27] Bone is also suggested to be an electret due to the development of large polarization charges.[28,29] These electrical properties of bone guide in the development, growth and healing of fractures.[2,13]

2.1.2.1. Piezoelectricity in bone

As mentioned, human bone is suggested to be a piezoelectric material, i.e. the biological electrical charges are generated via external force.[20,23,30] These electrical charges facilitate bone reconstruction and repair.[31] It is also suggested that Wolff's law is closely associated to the electromechanical functionality of bone.[13] Marino and Becker[32] conducted the experiments on a section of natural human cortical bone sample to evaluate its piezoelectric coefficient. Further, the coefficient was evaluated in demineralised (having collagen content) as well as decollagenised (having apatite content) bone samples. It was concluded that piezoelectric behaviour in bone is majorly due to the collagen component, while mineral content nearly does not contribute to the piezoelectricity.[32,33] Earlier, it was suggested that piezoelectricity in bone is a result of collagen fibres slipping over one another on the application of stress and thereby, generating the charges which further facilitates in growth and development.[23,33] Overall, it was suggested that non- piezoelectricity of the mineral apatite in bone is due to its centrosymmetric structure.[34] Collagen, on the other hand possesses non-centrosysmmetric structure.[33] However, it cannot be solely expressed that apatite constituent does not contribute to the piezoelectricity in bone. In the similar study, it has been observed that the piezoelectric coefficient is dependent on the angle between the direction of stress and bone axis.[20] It is reported that stress applied at an angle of 45˚ with the bone axis resulted in maximum piezoelectric coefficient.[20] The collagen fibres are oriented parallel along the direction of the bone axis and therefore, only piezoelectric coefficients d_{14} and d_{25} (equal and opposite to d_{14}) have non zero values.[2,20] The first subscript in the

piezoelectric coefficient (*i* in d_{ij}) represents the direction of generated electrical stimulation and second subscript (*j* in d_{ij}) depicts the direction of stress applied.[2,20]

The electric potential, generated in the bone is highly dependent on applied mechanical stress.[35] It was reported that in the areas where bone exhibit growth and repair, electronegative potentials act as the driving force.[35] It is also the area where bone undergoes compressive force whereas tensile force leads to electropositive potentials.[35] These potentials are different from the bioelectric potential of the bone. The bioelectrical signals appear on the fractured site of bone with negative polarity. These negative charges, in turn, activate the osteoblasts cells (bone-forming cells) for proliferation which results in healing of fractures as well as bone growth.[33,36] The positively polarized region of bone influences the osteoclasts cells (bone-resorbing cells).[33,36] Overall, bone is porous tissue having fluids which contribute to the transport of ions and nutrients to various regions of bone. It is reported that the electromechanical phenomenon in wet bones is associated with these fluids and is known as streaming potential.[26,33] The micropores of the bone are filled with charged fluids and there is an established interface between the charged walls of the bone and ions in the fluids.[33] Under mechanical deformation, these fluids tend to flow against the oppositely charged walls and consequently, the spatial distribution of charges is developed along the stream of fluid.[33] This spatial distribution of charges leads to a potential difference which is termed as streaming potential.[33] Therefore, bone *in-vivo* is considered to have piezoelectricity as well as streaming potential which co-ordinately induces growth, healing and development of bones.[33,37] These phenomenons are associated with the electromechanical as well as electrokinetic response of bone.[33,37] The maximum piezoelectric coefficient of bone is reported to be 0.7 pC/N.[38]

2.1.2.2. Pyroelectricity in bone

Pyroelectricity in bone was first observed by S B Lang in 1966.[24] It is the temperature-dependent phenomenon where the potential differences/charges are developed due to the

change in temperature of the bone. From the crystallographic point of view, it can be visualized as a unit cell having a polar structure which develops a potential difference between various faces in a crystal in response to change in temperature. Generally, solids having a lack of centre of symmetry as well as only one axis of symmetry exhibits pyroelectric behaviour. The non-centrosymmetric structure of collagen means that the pyroelectric effect in bone is due to the collagen component. Pyroelectric materials also exhibit piezoelectricity. This overall confirms that bone is piezoelectric. The pyroelectric coefficient of human femur has been evaluated to be $(3.6 \pm 2.1) \times 10^{-13}$ C cm^{-2} ºC in the temperature range of -25 ºC to 60 ºC.[24]

2.1.2.3. Ferroelectricity and electret nature of bone

Ferroelectric materials are subgroup of pyroelectric as well as piezoelectric materials. Ferroelectricity is an intrinsic property of bone as findings by El Messiery et al.[27] suggested, in which the hysteresis loop obtained for dry cortical human bone is comparable to the hysteresis loop of a moderate ferroelectric material [Fig. 2.3]. The report also suggested that the microscopic structure of bone is similar to that of a ferroelectric material in which domains containing permanent electric dipoles aligns/changes their direction on application of external electric field or mechanical stimulation. These domains attribute to the spatial distribution of collagen fibrils in the bone. These findings are also confirmed by Hastings et al.[39] Through thermally stimulated depolarization current (TSDC) measurement it has been reported that bone stores large polarization charges under electric field.[28,29] This confirms that bone is an electret material.

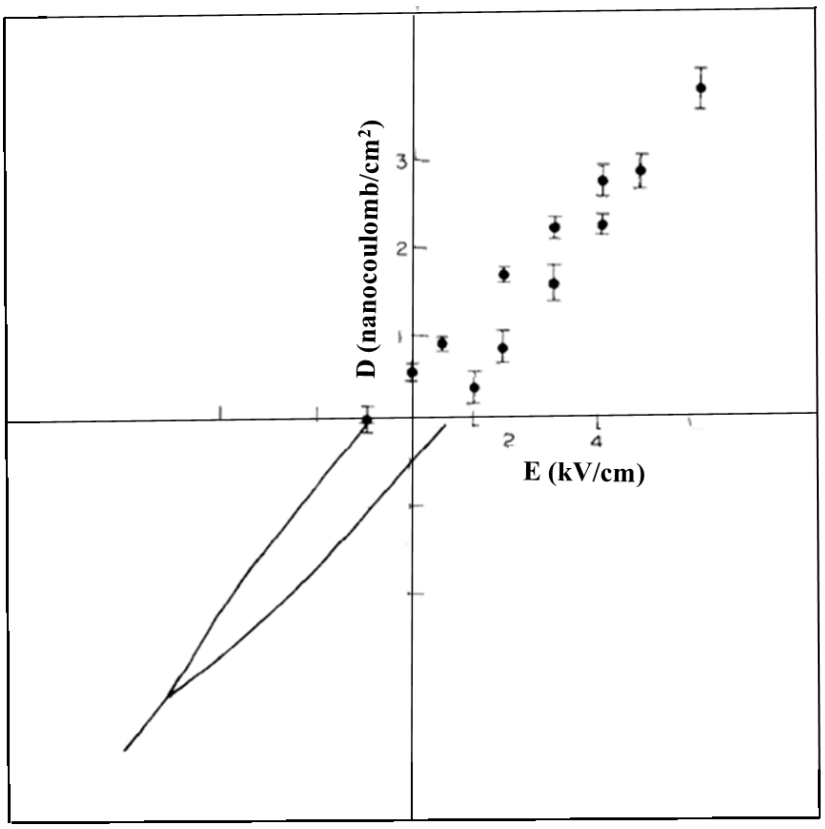

Fig. 2.3: Typical hysteresis loop for dry human bone specimen, representing ferroelectricity at 20˚C.[39] (Reproduced with permission from Elsevier)

In another report, to analyse the electret nature of bone, bone specimens were polarized with platinum electrodes in air with the field of 1.5 kV/cm at 25°C.[29] The TSDC curves of bone specimens consisted of 3 peaks at 100˚C, 300˚C and 500˚C. Each peak is associated with the polarization of certain composition in the bone i.e. lower temperature peak is analogous to collagen while peak at 300˚C is due to carbonate apatite and peak at 500˚C corresponds to hydroxyapatite.[29] Therefore, with these inherent electrical properties of bone it is expected that external electrical stimulation can affect the remodelling, growth and can heal fractures.[13] The selection for optimized parameters for electric field stimulation of bone requires basic understanding of interaction of electric field with bone cells. In the next section, a discussion on the need to develop a simplistic model for a generalized cell to understand the interaction of E-field is followed.

2.2. Introduction to the modelling of electrical equivalent of a generalized living cell

The electrical activity in the body, fundamentally originate from the living cells, smallest unit of any organism.[40,41] These electrical activities guide many physiological processes to maintain homeostasis (regulated substantial/elemental environment inside the organism) and protect cell from external environment. Overall, cell is composed of plasma membrane which is the outer protective sheet, separating intracellular compartment from extracellular matrix and various organelles. Cell membrane is made up of lipids and proteins [Fig. 2.4]. Proteins embedded in membrane provide pathways (for ions to flow) in the form of channels and pumps, while, lipids insulate the membrane. These two entities in the membrane metabolically protect cell from external environment. A cell membrane is polarized i.e., a small potential is maintained due to the uneven distribution of inorganic ions across it. This potential is also known as transmembrane potential (TMP).[40] While in resting state, cell maintains a fixed TMP through many processes of passive and active transports across it. However, in stimulated state, TMP is disturbed through many processes such as signaling, cell migration, cell division, differentiation, growth and healing processes. When these processes are complete, cell returns to the initial resting state. This potential is an essential indicator of the physiological state of the cell. The various inorganic ions, such as Ca^{2+}, Na^{+}, K^{+}, HCO_3^{-}, etc present in both intracellular as well as extracellular fluids are responsible for these cellular processes.[41]

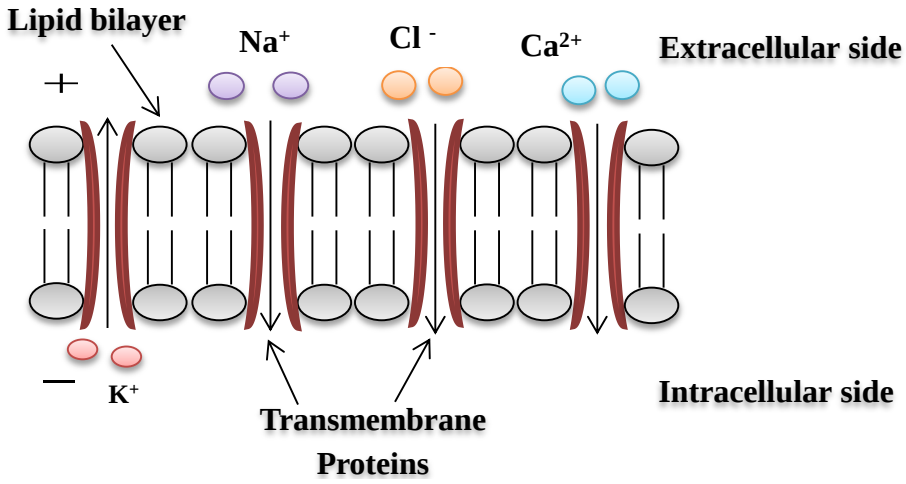

Fig. 2.4: Schematic representation of a cell membrane consisting of bilipid layer and proteins.

The polarized nature of cell membrane along with the chemical gradients induces endogeneous field/current. The endogenous electric fields play a critical role in the processes such as wound healing[14], growth and development of embroys[42], modifying cellular response[43] and modulating neuronal signalling.[44] Therefore, it is expected that the application of external E-field can effectively manipulate/guide the transport processes across cell membrane which can control various functionalities of living cells. In addition, living cells consists of various membrane bound organelles, together they maintain homeostasis through synchronized intracellular transport processes. Thus, the application of properly tuned external E-field parameters can also control intracellular processes.

At cell membrane level, the externally applied E-field leads to electroporation[45], necrosis, enhancement/inhibition in cell proliferation[46], transfer of chemotherapeutic drugs into cancerous cells, gene therapy[47], prevention of biofouling, bacterial decontamination and extraction of biomolecules.[48] While, intracellular effects includes programmed cell death and release of intracellular calcium ions from the endoplasmic reticulum, mitochondria and several other organelles which play an important role in cytoskeleton reorganisation, cell differentiation and cellular apoptosis etc.[49,50] The E-field induced intracellular effect also

termed as intracellular electro-manipulation,[51] can govern various transport processes across the membranes of intracellular organelles.[49] Multiple effects can be provoked depending on the E-field parameters such as strength, duration and no. of pulses applied as well as cell type.[52,53,54,55,56] For example, E-field strength of 5 kV/cm with pulse duration ranging from 0.4 μs to 1 μs or several (~ 100) milliseconds can be applied to obtain reversible electroporation while for irreversible electroporation, pulses in the range of milliseconds to seconds are required. On the other hand, for intracellular effects, E-field pulses in the nanoseconds range (600 - 10 ns) with higher strength (10 - 300 kV/cm) are required. However, these large strength and short duration E-field pulses also affects the cell membrane forming nanopores.[57] When the E-field is applied across the living cells, it disturbs the equilibrium and thus results in substantial increase in the flow of ions across the membrane and thereby TMP. E-field also causes structural/conformational changes in the proteins, lipids, as well as enzymes in the membrane along with thermal heating, electro-insertion and electrofusion.[58] Osteoblast cells, when exposed to external E-field, cellular migration also termed as galvanotaxis takes place.[59,60] In this process, simultaneous influx and efflux of Ca^{2+} takes place across the osteoblasts cells on the sides facing the electrodes and thereby cellular alignment along the field takes place. This alignment / cellular migration resulting from external E-field play a significant role in bone remodelling as well as osteoinduction.[61,62]

The interaction mechanism of E-field with single living cell has not been fully understood. However, number of attempts has been made to develop the theoretical understanding by designing the electrical equivalent of cell membrane.[63] Consequently, Deng et al.[64] also proposed the electrical equivalent circuit of single living cell considering nucleus as only organelle. The equivalent circuit of the living cell has been studied in other reported literatures also.[65,66,67] These studies considered cell and nuclear membrane to be a perfect

dielectric, which is not the realistic case. Cell membrane consists of ionic channels, pumps, transporters and other channels which mediate the flow of ions across it, while nuclear membrane consists of pores which pass selective molecules to be swapped across cytoplasm and nucleoplasm. Ellappan and Sundararajan[68] proposed the electrical equivalent of living cell by considering cell membrane to be a leaky dielectric and nuclear membrane to be a perfect dielectric.

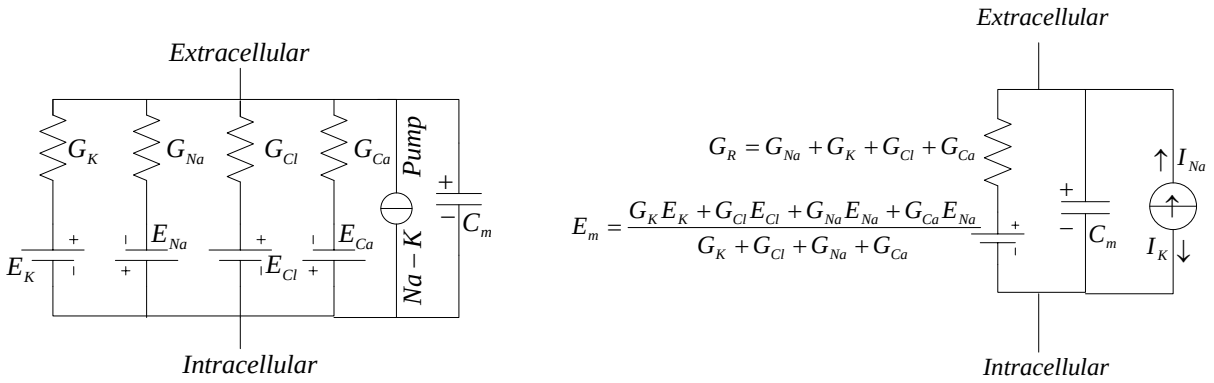

Fig. 2.5: (a) Parallel combination of voltage gated channels of Na^+, K^+, Ca^{2+}, and Cl^-, represented as a series combination of resistance and a battery, Na-K pump represented as a current source and a lipid bilayer represented as a capacitor, (b) electrical equivalent circuit of a cell membrane.

However, these studies focused on the dielectric properties of the membranes and conductive properties were feebly observed. The membrane conductive proteins allow different ionic currents across the cell membrane, while pores in nuclear membrane permits the selective molecules to pass across it. The change in the behaviour of the currents can considerably influence the cellular functionalities. Therefore, present study considers the simple electrical equivalent of living cell with cell and nuclear membranes acting as leaky dielectric [Fig. 2.5]. These are represented as the parallel combination of resistor and capacitor. Resistor in the cell membrane is suggested to be mimicking the behaviour of voltage gated channels, while

in nuclear membrane it is a symbolized behaviour of pores. In Fig. 2.5, additional circuit component, representing the behaviour of Na-K pump is also included in the circuit of cell membrane. However, it has not been included in the present study because under the influence of E-field, voltage gated channels are the main functioning unit. Under the application of E-field, ions traverse the least resistance path, which can be represented as the two electrical equivalent circuits (presented in chapter 3). The time constant of the circuits has been evaluated and its variation with various cellular adaptation processes has been analytically studied. The E-field strength required to electroporate the cell has also been calculated, assuming various critical TMPs. Using MATLAB simulations, models were also analysed with different pulsed voltage input signals of various durations.

2.3. Hydroxyapatite

Hydroxyapatite (HA) is a type of calcium phosphate which is structurally, chemically, morphologically and compositionally similar to mineral apatite of human hard tissue.[69,70] Calcium phosphates are of biological interest, which occur in six different phases such as hydroxyapatite (HA), dibasic calcium phosphate dihydrate (DCPD), dibasic calcium phosphate (DCP), monobasic calcium phosphate (MCP), β-tribasic calcium phosphate (β-TCP) and octacalcium phosphate.[71] Among these, hydroxyapatite (HA) has been recognized as a potential biomaterial due to its close structural and chemical similarity with the natural apatite as mentioned above. Also, most of the inorganic ingredients of bones and teethes are comprised of HA.[72,73] The implantation of synthetic HA demonstrates spontaneous osteointegration with bone.[70,74,75,76] HA is broadly utilized in bone grafts and prosthetic coatings.[77] In addition, application of HA also includes as fillers, drug delivery systems, protein chromatography, DNA separation etc.[78,79,80] Recently, it has been demonstrated that HA particulates also prevent the growth of cancer cells.[81]

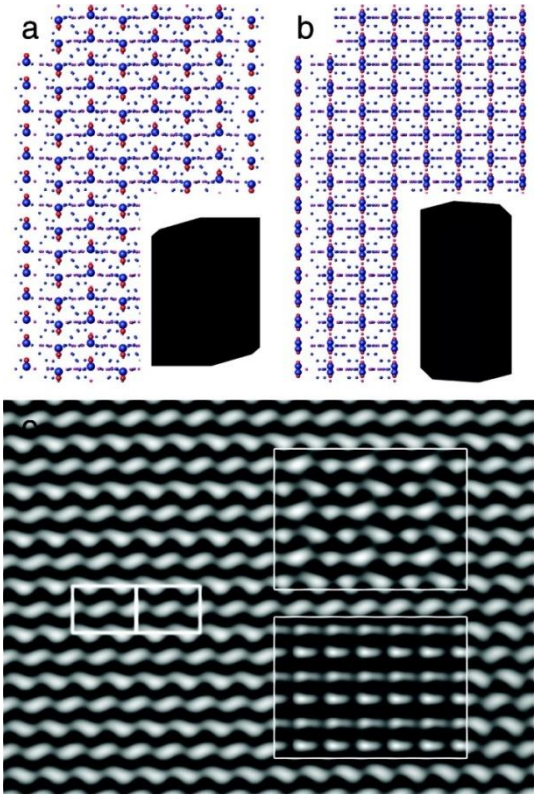

Fig. 2.6: a) Schematic illustrating the monoclinic hydroxyapatite (HA) with space group *P2$_1$/b* along [110] direction, b) Hexagonal HA with space group *P6$_3$/m* along [$\bar{1}$100] direction. In both the structures, the orientation of hydroxyl (OH^-) ions is different, c) Two-dimensional enlarged high resolution transmission electron microscopic image of monoclinic HA along [$\bar{1}$110] direction (upper inset) as well as hexagonal HA along [100] direction (lower inset), and a unit cell of HA (left inset) respectively.[82] (Reproduced with permission from American Chemical Society)

HA exists in hexagonal (space group: *P6$_3$/m*)[83] as well as in monoclinic (*P2$_1$/b*)[84] phases [Fig. 2.6]. Both structures consists of PO_4^{3-} tetrahedra along with Ca^{2+} ions which occur in two different positions, which is generally marked as Ca(I) and Ca(II).[82] The Ca(I) are arranged at interstitial sites and Ca (II) are located at the corners of equilateral triangle. The centre of the equilateral triangle is occupied by the OH^- ions, arranged uniaxially along c-axis. The difference between the two structures arises from the orientation of OH^- ions. In monoclinic

HA, the orientations of the OH^- ions are all up or down in the given column while in the adjacent column its orientation is opposite [Fig. 2.6(a)]. In hexagonal HA, with space group of $P6_3/m$, the OH^- ions are arranged in 2-fold disorder[82] i.e., orientations of adjacent OH^- ions are opposite in the same column [Fig. 2.6(b)]. However, this arrangement would develop steric interference[82] between the adjacent OH^- ions, therefore, hexagonal HA mostly contains vacancies of the OH^- ions. Hexagonal HA also forms during normal processing conditions which promotes formation of Ca^{2+} defects, OH^- vacancies and foreign/impurity ion inclusion rendering the orientation of OH^- ions in highly disordered manner along c-axis.[85]

It is considered that monoclinic HA is thermodynamically the most stable structure at room temperature having ordered alignment of OH^- ions in the lattice with negligible OH^- defects.[82,86,87] However, it is a highly stoichiometric structure which is unlikely to form during normal processing conditions.[84,86,88,89,90] Whereas, order-disorder (2 fold disorder) alignment of OH^- ions along with small amount of OH^- defects makes hexagonal HA lattice, the most stable structure at room temperature.[82,91] The occurrence of HA in monoclinic form was realized much later than the hexagonal HA because of the subtle difference between the structures.[82] The single crystals of chlorapatite [$Ca_{10}(PO_4)_6Cl_2$] whose structure is typical of monoclinic phase, consists of Cl^- ions centered around planar Ca^{2+} triangles, similar to the position of hydroxyl ions (OH^-) in hexagonal HA.[84,88] These single crystals of chlorapatite, under the steam of oxygen at 1200˚C, transforms to single crystals of monoclinic HA.[88] It is well known that the monoclinic HA structure transforms reversibly to hexagonal HA at about 210˚C.[92,93,94] This phase transformation occurs due to ordered orientation of the hydroxide (OH^-) ions along c-axis which becomes highly disordered at elevated temperatures and also induces OH^- defects.[85]

Fig. 2.6 (c) represents the high resolution transmission electron microscopic image (HRTEM) of HA. The insets depict the simulated images of the structures of HA. The upper right inset

represents monoclinic HA along [110] and the lower right inset depicts hexagonal HA along [$\bar{1}$100]. The upper inset portrays high similarity with the monoclinic HA in Fig. 2.6 (a). While, in lower inset, significant difference can be depicted with respect to hexagonal HA in Fig. 2.6 (b).

2.3.1. HA as an electret

Among its various striking features, HA can be converted into electrets by the application of external electric field (E-field) at elevated temperature.[95,96] The importance of HA electrets as an implant can be realized from the fact that under different loading conditions (compression, tension, cyclic, etc.), living bone generates charges on its surface which further assists in bone-growth/new-bone formation as well as bone fracture healing.[95,97,98,99,100] The rationale for electret formation at elevated temperature is elaborately described in the coming sections. These HA electrets display enhanced osteogenic capability as well as favour new bone formation.[101,102,103,104,105] In addition, the surface charge controls the interface between HA and living cells, *in vitro* and *in vivo*.[102,106,107,108,109,110] These surface charges influence the protein adsorption that further affects cell adhesion, migration, morphology and proliferation.[95,106,108] In addition, accelerated growth of bone like apatite on polarized HA in simulated body fluid has also been reported.[95,107] As far as the influence of surface polarity is concerned, osteoblast cells exhibits enhanced cell proliferation on negatively polarized surface of HA. [107,108,111] It has also been reported that the polarized surfaces induce new bone formation and enhanced osteobonding towards negatively charged surface from the site of injury.[112,113] In addition, polarized HA also promotes regeneration of blood vessel and epidermis during wound healing.[114,115]

The electret formation of HA can be realized based on the mobility of hydroxyl (OH^-) group, present in the c-axis column of the hexagonal lattice.[96] The protons (H^+) associated with the O^{2-} ions are weakly bonded at elevated temperature ($\geq$ 200˚C).[116] In the process, the

arrangement of the OH^- ions becomes highly disordered. Thereafter, under the application of E-field at elevated temperature, reorientation of the OH^- ions takes place along c-axis.[95] It is also known that at elevated temperatures ($\geq 700^{\circ}C$), protons (H^+) dissociate from the O^{2-} ions and conduct along c-axis. Therefore, HA is also considered to be as quasi-one-dimensional protonic conductor.[117,118,119] These ordered OH^- ions along c-axis behave as electric dipoles under the influence of external E-field at elevated temperature.[116] The direction of the aligned OH^- ions along c-axis behaving as electric dipoles can be reversed depending upon the polarity of the applied E-field.[120] The cooling of HA under continuous exposure of E-field freezes the OH^- dipoles. On removal of E-field, HA is rendered in its polarized state.[95,96] Thereafter, on reheating the polarized HA, the dipoles relax thermally, giving rise to depolarization current with respect to temperature which is also known as thermally stimulated depolarization current (TSDC).[121] However, along with OH^- dipoles, space charge is also developed in HA due to the proton (H^+) conduction.[91] Therefore, TSDC results due to the relaxation of dipolar as well as space charge polarization. The formation of HA into electrets is based on the polarization depolarization processes which has been discussed substantially coming sections.

As mentioned above, TSDC is the study of the temperature dependent dielectric relaxation in the solid electrolyte.[122,123] Through TSDC, dielectric losses occurring in the solid electrolyte can be measured in a very low frequency range (10^{-2}-10^{-4} Hz) which is the characteristic feature of TSDC.[124] In this method, sample is placed between the electrodes and simultaneously polarizing field (E_p) at elevated temperature (T_p) for a certain time (t_p) is applied. Thereafter, under constant application of E_p, sample is cooled down to room temperature. At room temperature, E_p is removed and the sample is again reheated at a certain heating rate (β) with the electrodes, connected to low current (ultralow) measuring device (such as electrometer, picoammeter, etc.). The measured discharge current is called

TSDC which is a function of temperature. The spectrum of TSDC is a combination multiple relaxation mechanisms, present in the sample.

These multiple relaxations can be split up into uncoupled distributions of Debye relaxation processes. The frozen polarization [*P(t)*] is then assumed to decay as,[125]

$$\frac{dP(t)}{dt} = -\frac{P(t)}{\tau(T)} \tag{2.1}$$

Where, $\tau(T) = \tau_o e^{\frac{E_a}{k_B T}}$, where, τ_o is the pre-exponential factor and E_a and k_B are activation energy for the relaxation of dipoles and Boltzmann's constant, respectively.[122] The depolarization current density, can then be expressed as a function of temperature as,

$$J(T) = \frac{P_o}{\tau_o} e^{\left[-\frac{E_a}{kT}\right]} e^{\left[-\frac{1}{\beta\tau_o}\int_{T_i}^{T_f} e^{\left[-\frac{E_a}{kT}\right]} dT\right]} \tag{2.2}$$

Where, $\beta = \frac{dT}{dt}$ is the heating rate; T_i and T_f are the initial and final temperatures of measurement. The eq. (2.2) can also be written in the form,

$$\frac{E_a}{kT} + \ln \tau_o = \ln\left[\frac{1}{\beta}\int_{T_i}^{T_f} J(T)dT\right] - \ln J(T) \tag{2.3}$$

The eq. (2.2) represents the current density due to the relaxation of the dipoles.[126,127] In the eq. (2.2), the first exponential is dominant at lower temperatures, which represents the increase in the TSDC with temperature. The second exponential dominates at higher temperatures which gradually counter the increase in TSDC until the maximum is reached. The TSDC spectrum is, therefore, symmetrical with respect to temperature. The activation energy (E_a) can be evaluated from the slope of the linear curve, plotted between *ln τ* v/s *1/kT* from the eq. 2.3.

TSDC is a high resolution dielectric characterization technique because of its low frequency equivalent which is given as,[124]

$$f = \frac{E_a \beta}{2\pi R T_m^2} \tag{2.4}$$

Where, R is the ideal gas constant, T_m is the temperature at which the maximum depolarization current density peak is observed. The given low frequency equivalent enhances the separation between different relaxation peaks in the TSDC spectra on the temperature axis. The advantage in the TSDC methodology is the separate stages of polarization and depolarization experiments compared to other dielectric measurements in the given frequency domain where dipolar relaxations are often overlapped with the ionic conductivity in the sample. A detailed discussion on the TSDC is followed up in chapter 4.

2.3.2. Origin of electrical nature of HA

Electrical properties of HA are highly influenced by the lattice hydroxide (OH^-) ions oriented along c-axis at the centre of Ca^{2+} triangles.[117] In addition, it has been suggested by Nagai et al.[128] that the surface of HA is ionic in nature and therefore, binds with polar molecule such as water. These water molecules give rise to proton mediated conduction at low temperatures.[129,130] At elevated temperature (> 200˚C), it is considered that the protons (H^+) of the hydroxyl (OH^-) group at the OH^- site has a tendency to dissociate and become mobile.[117] As a consequence of which, water molecule releases from the lattice, i.e., one OH^- ion at OH^- site combines with the proton (H^+) on the other OH^- site. In the process, HA develops large number of defects in OH^- columns without disturbance of the apatite structure.[117,131,132] As a consequence, one OH^- ($V_{OH}^{\bullet}$) vacancy and one proton vacancy (V_H') is created. This process of dehydration of the lattice hydroxide ions is described as,

$$Ca_{10}(PO_4)_6(OH)_2 \rightarrow Ca_{10}(PO_4)_6(OH)_{2-2x}O_x\square_x + xH_2O\ (g)$$

$$\text{Or} \tag{2.5}$$

$$OH^-_{OH} + OH^-_{OH} \rightarrow O^{2-}_{OH} + \square_{OH} + H_2O\ (g)$$

Where, $\square_{OH}$ indicates a vacancy at the OH^- lattice site and $O^{2-}{}_{OH}$ is the converted oxide ion when proton (H^+) is dissociated from it. Therefore, due to mobile nature of protons (H^+) bounded to O^{2-} in the OH^- columns, one-dimensional proton conduction takes place through the c-axis columns.[117,118,119,133] In addition, it has been reported that the majority of charge carriers present in HA are protons (H^+) which has been recognized by hydrogen concentration cell at 900˚C.[117] The protonic conductivity has been found to be almost 10^{-3} $S.cm^{-1}$ at 700˚C.[117] The proposed one-dimensional conduction path along c-axis consists of vacancy at OH^- site which can hinder the conduction of protons (H^+).[117] Also, the distance between adjacent OH^- site is too long (0.344 nm) and that of between OH^- site and $(PO_4)^{3-}$ tetrahedral is 0.307 nm, which is comparatively short.[132] Therefore, the possibility to form hydrogen bond between the hydrogen of OH^- ions and oxygen of $(PO_4)^{3-}$ ions is obvious.[117] Considering this conduction path of protons to be likely suitable for dehydration process, which is as follows,

$$OH^-{}_{OH} + OPO_3{}^{3-} + OH^-{}_{OH} \rightarrow O^{2-}{}_{OH} + H\ldots OPO_3{}^{2-} + OH^- \rightarrow$$

$$O^{2-}{}_{OH} + OPO_3{}^{3-} + H\ldots OH_{OH} \rightarrow \qquad (2.6)$$

$$O^{2-}{}_{OH} + OPO_3{}^{3-} + \square_{OH} + H_2O\ (g)$$

The proposed conduction mechanism forms defects at OH^- site which can be suppressed by supplying H_2O vapour in the sintering environment of HA.[134] Further, it has been reported, through various processing conditions, that Ca^{2+} defects may form in HA.[135] Using density functional theory (DFT) for defect formation energetics, it has been evaluated that for compensating the charge of defect at Ca^{2+} site, proton interstitial exists.[136] These interstitial protons likely form bond with the OH^- ions in the c-axis and thereby, additional conduction through proton interstitial hopping takes place in Ca^{2+} deficient HA.[131] The instability of the protons (H^+) along c-axis of HA at elevated temperature indicates various polarization

mechanisms which are discussed further in the subsequent section. In addition, its orientation also gives an impression of the ferroelectric nature of HA.

2.3.3. Mechanism of polarization and depolarization in HA

The polarization and depolarization in HA occur due to thermal flip flop of OH^- dipoles, present along columnar c-axis.[95,96,117,137] This is due to the fact that protons (H^+) attached to O^{2-} ions in OH^- becomes activated in the temperature range of 200˚C - 300˚C.[95] At elevated temperatures (≥ 800˚C), these protons (H^+) are predominantly dissociated from the OH^- ions which combine with the OH^- ions at another OH^- site to form water of hydration which results in dehydroxylation of the lattice OH^- ions.[138] Hitmi et al.[116,139,140] studied the dielectric relaxation properties of HA through TSDC measurements. It has been suggested that the protons (H^+) rotate or relocate themselves around O^{2-} ions in response to thermal energy. This model is called the proton rotation model. This thermally stimulated movement of protons around O^{2-} ions in the columnar c-axis initiates phase change from monoclinic to hexagonal at approximately 211˚C.[92,93] The phase transition is attributed as quasi-statically stabilized phase transition in which the thermal motion of protons (H^+) around O^{2-} ions depends on the adjacent OH^- ions along c-axis.[116,139,140] Another mechanism for polarization and depolarization can be attributed to ionic transport of H^+, O^{2-} and OH^- ions in the HA lattice. The proton (H^+) migration takes place along OH^- channels which is associated with the activation energy of about 1 eV.[96] It involves reorientation and migration of protons (H^+) to the adjacent proton-vacancy site (O^{2-}). The protons (H^+) can also migrate via nearest tetrahedral PO_4^{3-} ions.[117] However, the protons, which are weakly attached to the OH^- ions, dissociate directly to conduct along c-axis.[141]

It has been suggested that polarization and depolarization processes in HA are highly dependent on polarizing temperature (T_p). The lower T_p (≤ 400˚C) yields polarization through proton (H^+) migration via adjacent OH^- ions as,[141]

$$OH^- + OH^- + OH^- + OH^- = OH^- + O^{2-} + OH^- + HOH \quad (2.7)$$

At higher T_p (≥ 500˚C), the diffusion of O^{2-} ions in the structure due to partial dehydroxylation of HA at elevated temperature (> 500˚C) contribute to the polarization.141 The partial dehydroxylation takes place as,

$$OH^- + OH^- + OH^- + OH^- = O^{2-} + \square + OH^- + OH^- + H_2O\ (g) \quad (2.8)$$

Where, □ denotes the vacancy of an OH^- ion. The migration of O^{2-} ions takes place through these vacancies. The activation energy evaluated for their diffusion/migration is about 2 eV.[142] However, activation energy higher than 2 eV is associated with the migration of OH^- ions.[143]

Dehydroxylation induces defects (OH^-) in the HA structure at high temperatures (≥ 800˚C). It has been reported that as the defect (OH^-) concentration increases, the dipole and space charge polarization also increases.[144] Also, from the TSDC spectra of defect induced HA, polarized at high temperature (~ 400˚C) and low electric field (~ 1 - 4.5 kV/cm), it was concluded that the peak having a linear increase in its peak current density (J_{max}) with the polarizing field (E_p) is attributed to dipolar polarization, while an exponential increase in peak current density is attributed to space charge polarization.[124,145,146,147] The activation energies, corresponding to the dipolar and space charge polarization in defect induced HA lie in the range of 0.6 eV - 0.9 eV and 1.01 eV - 1.02 eV, respectively.[144] In defect induced HA, the dipolar polarization is proposed to be based on the mechanism of formation of defect dipoles due to vacancies of OH^- ions as well as H^+ at OH^- ions sites along the c-axis in the lattice.[144] With the increase of defect concentration, the defect pair dipole increases and henceforth the dipolar polarization also increases.[144] However, this dipolar polarization is different from the reorientation of the OH^- dipoles which is suggested to be the fundamental origin of dipolar polarization in HA.[116]

Similarly, space charge polarization in defect induced HA is majorly associated with grain boundaries.[144] Under the influence of E-field, protons (H^+) conduct through defects in grain and accumulate near the grain boundaries. This distribution gives rise to space charge polarization. As defect concentration increases, the density of the mobile protons increases with an increase in the number of proton vacancies, as a result, space charge polarization also increases. Therefore, it is suggested that persistent polarization in defect induced HA comprises of dipolar as well as space charge polarization, associated with the grains and grain boundaries.[142,144]

In another report, the surface charge density induced by the polarization process on the HA surface has been evaluated using Kelvin probe method.[148] In this method, sample is placed between the electrodes, where one electrode touches the surface of the sample, the other electrode is kept at a definite distance. The non-contact electrode vibrates resulting in the alternating current which is measured through ammeter. Also, a constant voltage source is connected in series with the present set-up. At a particular distance (*l*) between the electrode and the sample, when the resulting current is zero, a constant voltage bias is utilized to evaluate the surface charge density. The kelvin probe equipment is kept in vacuum chamber along with resistive heater to monitor the temperature of the sample.[149] It was realized that the surface of HA, which was polarized via positive bias voltage induce positive charges and the surface which was polarized with negative bias induce negative charges. This was however, different from the polarity of barium titanate (BT) which was polarized under similar conditions. It induced negative charge on the side of positive electrode and vice versa. This is due to the phenomenon of spontaneous polarization in BT, which can be reversed on the application of the field.[150] The spontaneous polarization in BT is due to the crystal distortion in which oxygen (O) and titanium (Ti) ions are displaced with respect to the barium (Ba) ion in the unit cell.[150]

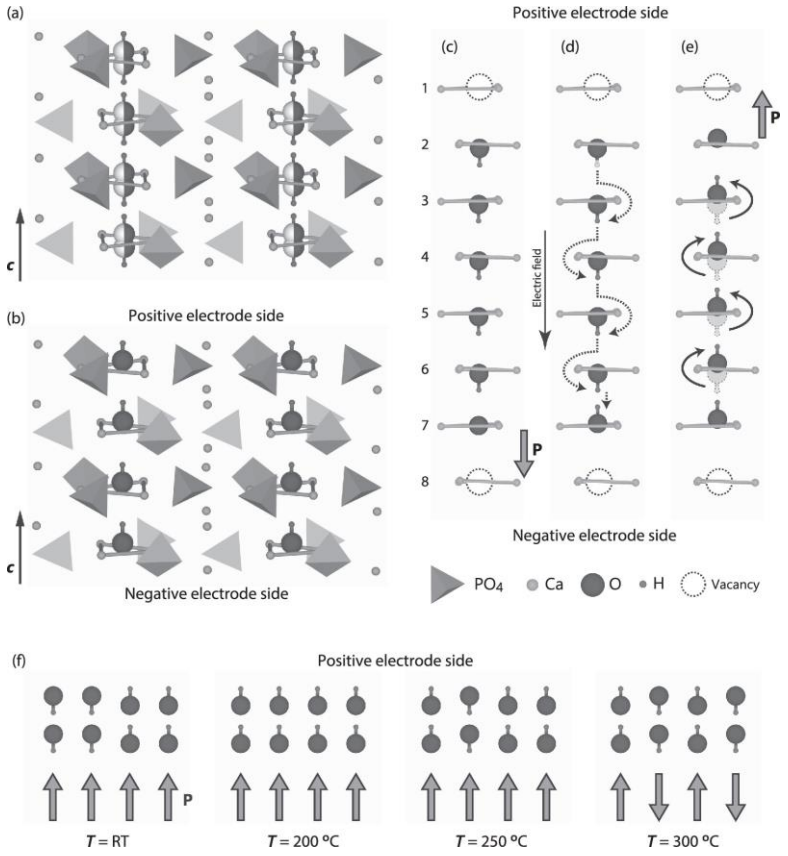

Fig. 2.7: (a) Hexagonal lattice of HA with order-disorder arrangement of OH^- ions, (b) depicts the Polarized HA, (c) - (e) represents the mechanism of formation of surface charges via proton (H^+) migration as well as reorientation of defect dipole polarization under the application of E-field. (f) Orientation of OH^- ions as well as of defect dipoles at different temperatures.[149] (Reproduced with permission from AIP publishing)

It has been concluded that surface charge density on HA surface is due to the dipolar polarization as the associated activation energy evaluated was 0.69 eV which is attributed to the dipolar polarization in defect induced HA.[91] The surface charge density on HA is independent of the sample thickness which further confirms the existence of dipolar polarization in HA.[149] It has been also concluded via water immersion test that the surface charge density on HA is mainly due to the dipolar polarization.[149] This test also confirms the thermal stability of the existing dipolar polarization in the sample.

The schematic representation in Fig. 2.7 depicts the mechanism of formation positive surface charges on the side of the positive electrodes on HA surface and vice-versa.[149] Fig. 2.7 (a) depicts the typical arrangement of OH^- ions in the hexagonal structure of HA. In Fig. 2.7 (c), OH^- vacancies are present in the lattice due to the high temperature sintering. In addition, these defects lead to the formation of defect dipoles. When the electric field is applied at high temperature, protons migrate to the adjacent OH^- sites and therefore results in the reorientation of the defect dipoles, as depicted in Fig. 2.7 (e). The process of proton migration as well as reorientation of defect dipoles results in the formation of surface charge.[151]

Fig. 2.7 (f) depicts the reorientation of the OH^- ions at different temperatures. It can be observed that at room temperature (RT), in polarized HA, the orientation of OH^- ions can be disturbed by interaction with the water molecules or by polishing process which induces stress in the sample. However, when the sample is heated, HA starts to regain its polarization to the original value. Thereafter, when the phase transition temperature (~ 210˚C) is reached, the polarization starts to decay with further increase in temperature. It is also reported that the surface charge measured through Kelvin probe experiment is almost four orders less than the polarization evaluated from the TSDC curve.[91,149] This can be due to the fact that TSDC measurement supposedly evaluates all the charges formed in the sample such as trapped charges at the grain boundaries and all the other volumetric charges.[149]

2.3.4. Ferroelectricity in HA

Ferroelectricity is the property of the material which possesses reversible spontaneous polarization.[152] The hydroxide (OH^-) present along c-axis column imparts distinct electrical properties to HA such as proton conductivity,[117,132,153,154] electret formation[95,96,148,155] and ferroelectricity.[87,152,156,157,158,159,160,161] Among these, ferroelectricity is associated with the monoclinic phase of HA.[162] The monoclinic phase of HA (space group: $P2_1/b$) is a highly stoichiometric phase with ordered alignment of OH^- ions along c-axis.[84,82] The structure is

said to be 'antiferroelectric-like' as the alignment of the OH^- ions in one column is opposite to the alignment of the OH^- ions in the adjacent column.[120] This type of structural ordering of OH^- ions is related to the presence of ferroelectricity in HA.[152,119,154,156,160] However, polarization-electric field (P-E) hysteresis loop does not indicate the presence of the ferroelectricity in HA.[162] In the dielectric behaviour of HA with temperature, minor anomaly is observed around 210˚C, which is suggested to be associated with the monoclinic (space group: $P2_1/b$) to hexagonal (space group: $P6_3/m$) phase transition.[92,93,94,163,164] This anomaly occurs when the ordered alignment of OH^- ions along c-axis becomes highly disordered. Both of these structures are electrically non-polar as they are centrosymmetric around OH^- ions, oriented along c-axis.[156] On these grounds, the polar phase of HA cannot exist. However, thermally stimulated depolarized current studies suggest the existence of polar phase of HA.[96] Based on this, Tofail et al.[156] suggested that the presence of temperature dependent dielectric anomaly at almost 210˚C is due to antiferroelectric to ferroelectric phase transition i.e., non-polar monoclinic ($P2_1/b$) to polar monoclinic ($P2_1$) or hexagonal ($P6_3$) phase. These polar phases possess no centre of symmetry which was earlier reported by Havery et al.[87]

Figs. 2.8 (a) and (b) represent the non-polar monoclinic phase ($P2_1/b$) having the ordering of the hydroxyl (OH^-) group along c-axis in antiferroelectric type. In addition, the non-polar monoclinic phase having minimum energy is thermodynamically the most stable structures of HA. The polar phase of HA is associated with the unidirectional ordering of OH^- ions along crystallographic c-axis ([001]) which indicates the ferroelectric ordering. The polar monoclinic ($P2_1$) as well as hexagonal ($P6_3$) phases have slightly higher energy (few kJ/mol) as compared to the non-polar monoclinic phase ($P2_1/b$). Therefore, either stabilization of the polar phase of HA takes place or results in non-polar to polar phase transition. Chaiti et al.[165] reported the stabilization of HA surface (001) with a needle type structure having a cylindrical axis due to presence of ordered OH^- ions. The cylindrical axis is presumed to be

crystallographic c-axis having ordered OH^- ions depicting ferroelectric ordering, which are surrounded by Ca^{2+} triangles. This structure is, therefore, inserted in a dielectric medium of interstitial Ca^{2+} ions and PO_4^{3-} tetrahedra. Based on these studies, nanocrystalline HA depicts ferroelectricity and has been experimentally revealed using piezoresponse force microscopy.[152]

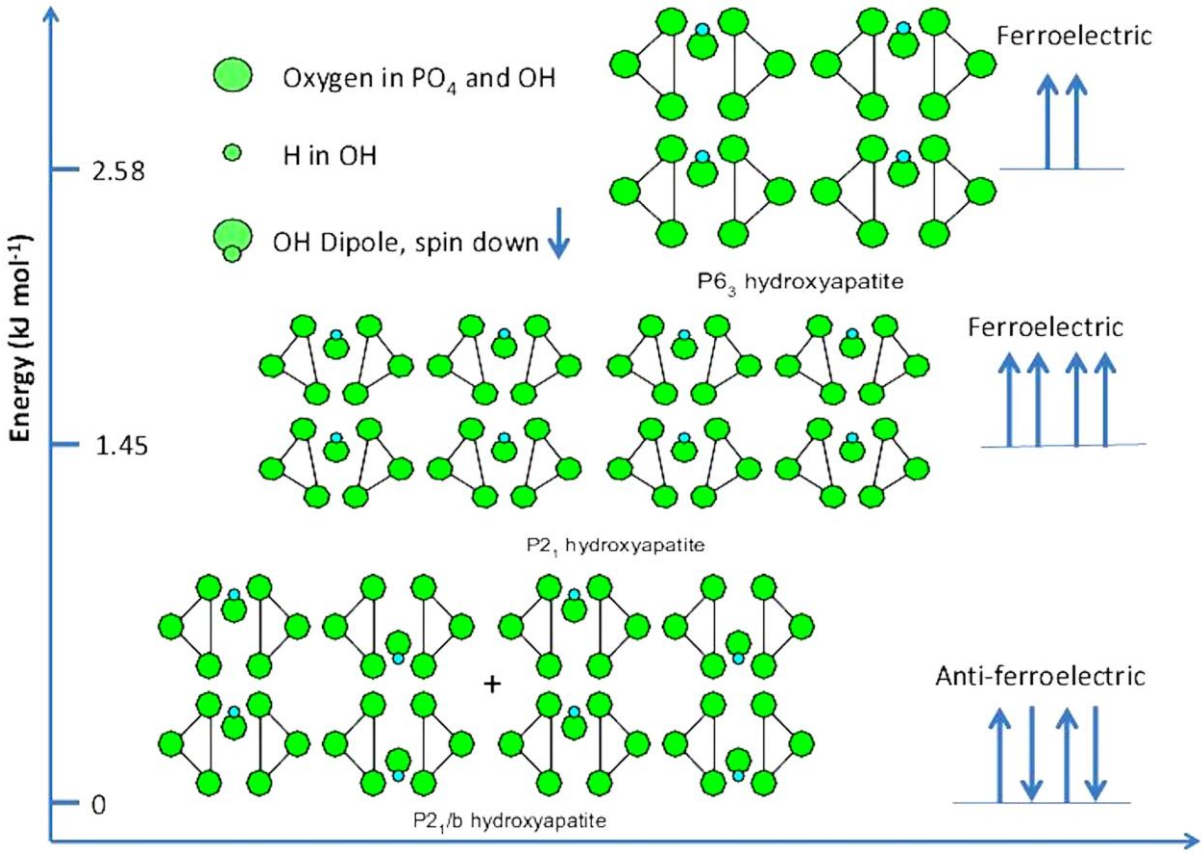

(a)

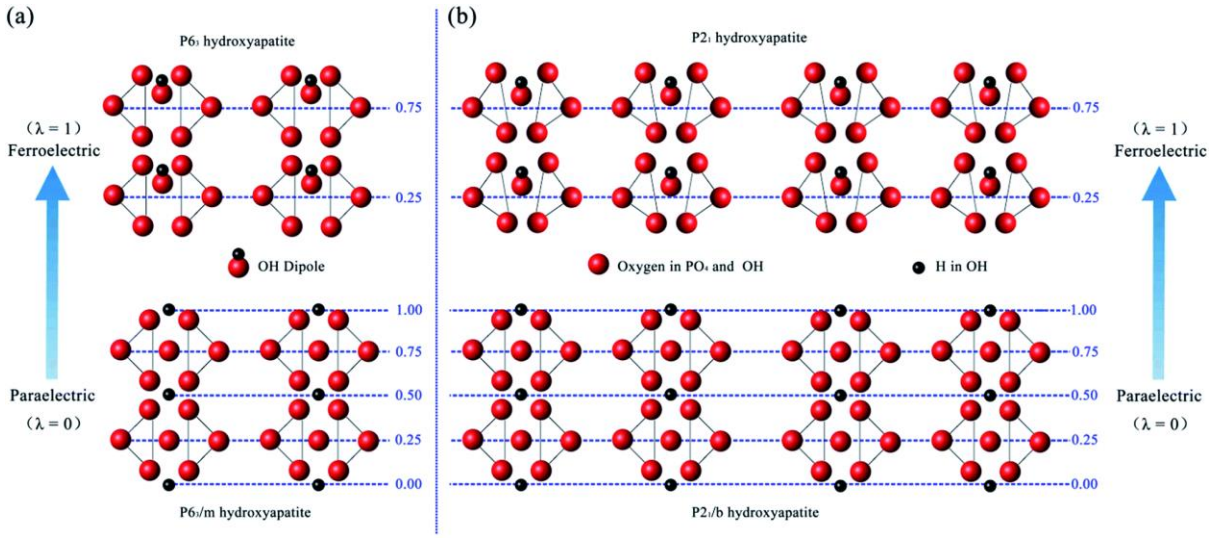

(b)

Fig. 2.8: Schematic illustration of the orientation of the hydroxyl (OH^-) ions with respect to Ca^{2+} triangles.(a) Energy scale of the non-polar *$P2_1/b$* monoclinic phase, polar *$P2_1$* monoclinic phase and polar *$P6_3$* hexagonal phase, (b) phase transition from paraelectric to ferroelectric phase. The paraelectric phase is depicted as the *$P6_3/m$* hexagonal as well as *$P2_1/b$* monoclinic phase.[85,152] (Reproduced with permission from Springer Nature)

Further evidence of the ferroelectricity in HA is suggested to be based on the TSDC spectra of its monoclinic counterpart [Fig. 2.9]. In the spectra sharp current peak is observed at the phase transition temperature (~ 210˚C) i.e., monoclinic to hexagonal.[162] Similar sharp current peaks are observed in ferroelectric materials on their depolarization.[166,167,168] Although, the intensity of the sharp peak is low, nevertheless, it suggests the presence of ferroelectricity in HA. In addition, these similar sharp current peaks were not present in the TSDC spectra of hexagonal (*$P2_1/m$*) HA.[91,96,116,139,169,170,171] The spectra consisted of one sharp peak (peak A) and two broad peaks (peak B and peak C). The first broad peak (peak B) is mainly associated with the reorientation of the OH^- dipoles as the activation energy associated with it, is about 0.4 eV.[116,169] The values are almost independent of the parameters such as polarizing temperature, field and time. The second broad peak (peak C) is analogous to the space charge

polarization due to proton conduction in grain boundaries.[91,96,169] The sharp peak (peak A) depicts the phase transition in which only 1% of the total polarized OH^- dipoles, depolarizes diffusively which is indicative of the ferroelectricity in HA [inset of Fig. 2.9(a)].[162] As mentioned above, the ferroelectricity is mainly associated with the ordering of the OH^- ions along c-axis. However, this ordering generally breaks and results in the short lengths of the clusters, formed by the OH^- dipoles along c-axis. The breakdown is due to the dehydration process as well as calcium defects which results in OH^- vacancies.[162] Due to these short length clusters of OH^- dipoles along c-axis, ferroelectricity is hard to observe in HA. The long OH^- chains along c-axis exhibits ferroelectricity and is rarely present.

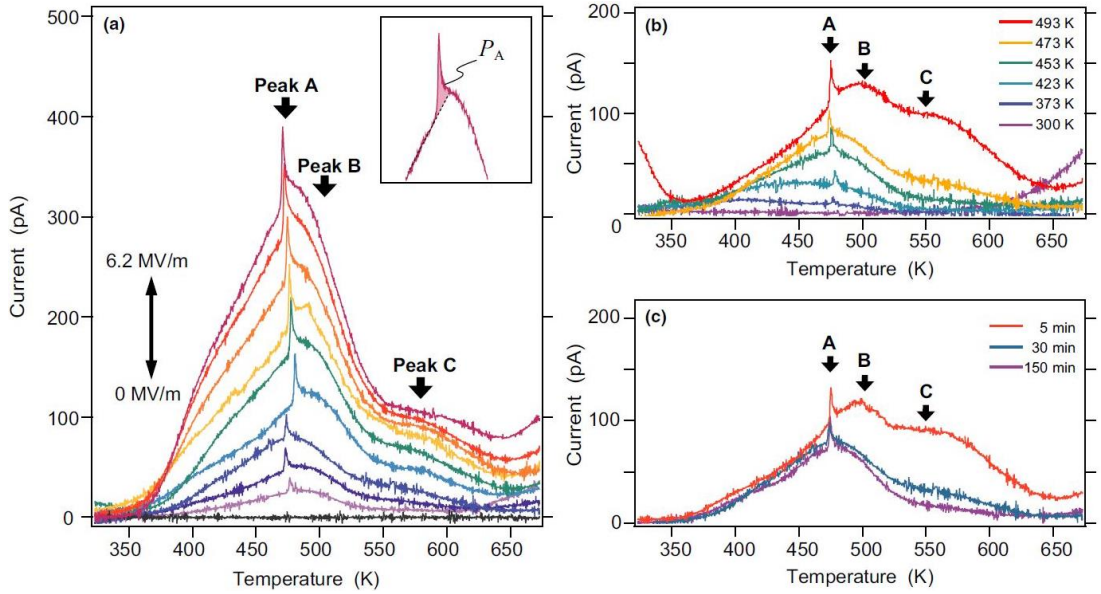

Fig. 2.9: TSDC spectra of polycrystalline monoclinic HA with different polarization parameters such as polarizing field (E_p), polarizing temperature (T_p) and polarizing time (t_p). (a) E_p = 0 - 6.2 MV/m, T_p = 473 K, t_p = 30 min. (b) E_p = 1.5 MV/m, T_p = 300 - 493 K, t_p = 30 min. (c) E_p = 1.5 MV/m, T_p = 473 K, t_p = 5 - 30 min. The inset in (a) depicts the polarization P_A (area of the sharp peak).[162] (Reproduced with permission from John Wiley and Sons)

Due to the consideration of the non-centrosymmetric structure of HA ($P2_1$; $P6_3$), piezoelectricity might be present at macroscopic level which was recently established by Tofail et al.[158] The measurement was carried out by quasistatic direct measurement[172,173,174,175] and ultrasound interference methods.[176,177] Both these methods are well established and standard to measure to piezoelectricity at a macroscopic level in a polycrystalline material.[178] The measured d_{31} coefficient in HA is almost 6.84×10^{-18} C/N which is almost 6 orders less than that for general PZT ceramics.[158] The low values have been suggested to be associated with the lack of anisotropy in HA. Although, powder diffraction revealed the presence of piezoelectric phase but thereafter on sintering, development of defects and the presence of pores might have reduced the anisotropy in HA.[87] However, the individual grains in the polycrystalline HA may exhibit piezoelectricity, and therefore piezoelectricity can be established at a nanoscale dimension.[152]

It has been suggested that on polarizing HA, it is converted into electrets having induced surface charges.[96,169] These surface charges have been reported to enhance the formation of bone apatite when immersed in simulated body fluid (SBF).[95] In addition, the developed surface charges on polarized HA, facilitate increased osteobonding.[104] Natural bone induces surface charge, owing to temperature gradient.[24] The induction of surface charge with temperature change and vice versa is pyroelectricity.[24] This property of bone, helps in its growth and development. The consideration of non-polar to polar phase transition at higher temperature indicates HA might possess pyrolelectricity.[156]

Fig. 2.10 represents the concept of pyroelectricity in polarized HA.[157] The polycrystalline HA consists of polar as well as non-polar grains. The polar grains (arrows pointing in the same direction) indicate polar hexagonal ($P6_3$) or polar monoclinic ($P2_1$) phase having ordered OH^- ions along c-axis, aligning in the same direction. Non-polar grains with antiparallel arrows indicate non-polar monoclinic ($P2_1/b$) phase [Fig. 2.10 (a)]. On heating HA above its phase

transition temperature and thereafter polarizing it, polar grains start to reorient in the direction of applied field, while non-polar grains exhibits phase transition to polar phase [Fig. 2.10 (b)].

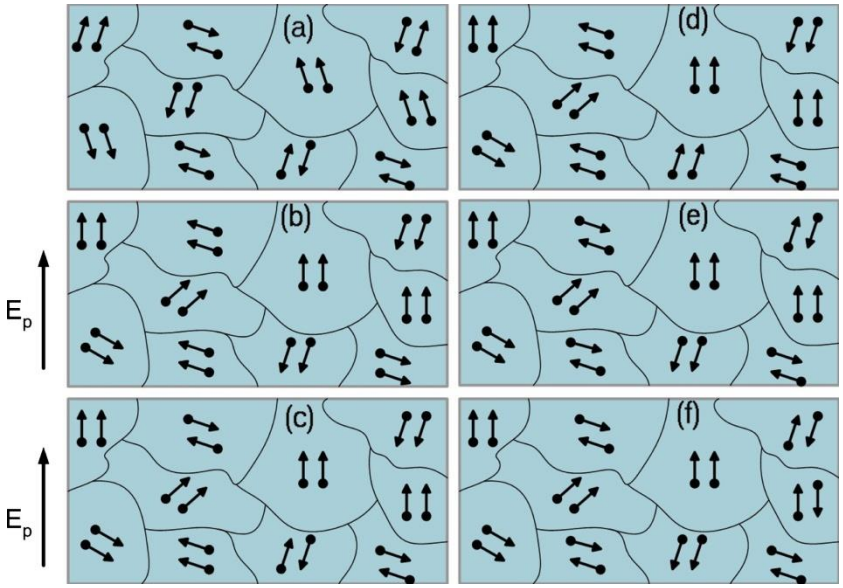

Fig. 2.10: Schematic representing the pyroelectric effect in the polycrystalline HA with non-polar and polar grains. Non-polar grains are represented as arrows in antiparallel orientation while parallel arrows represent polar grains.[157] (Reproduced with permission from AIP publishing)

On cooling to room temperature under the presence of polarizing field, some polar grains preserve their orientation while other returns to their equilibrium state of non-polar phase [Fig. 2.10 (c)]. On reheating (300˚C - 500˚C), the non-polar grains gain sufficient thermal energy and reorient into polar phase [Fig. 2.10 (d)]. This is the state of spontaneous polarization and therefore, depicts pyroelectricity. Thereafter, on cooling (500˚C - 300˚C), polar grains reorient to non-polar phase due to thermal flip-flop, although the net polarization is not zero [Fig. 2.10 (e)]. On further cooling to room temperature, most of the polar grains transforms to non-polar grains and therefore, the net polarization is zero [Fig. 2.10 (f)]. The TSDC spectra suggest that HA is pyroelectric in the temperature range of 300˚C - 500˚C.[157]

The pyroelectric coefficient ranges from 0.1 to 40 nC cm^{-2} K^{-1} in this temperature range.[157] The lower temperature (27˚C - 60˚C) pyroelectric coefficient ranges from 15 to 64 nC cm^{-2} K^{-1} which is almost four times higher with that of the observed in bone and tendon.[157]

2.3.5. Coupling of electro-active response and biocompatibility of HA

On induction of surface charges, HA electret gives rise to quasi permanent electric field near their surface.[148] The endogeneous physiological electric fields also play a vital role in cellular metabolic activities.[179,180] Therefore, it is expected that the coupled action of both the fields would induce favourable biological response. In addition, cell signalling[181] and charge on the material surface[182] are crucial in regulating cellular metabolic activities. It has been demonstrated that polarization results in the generation of surface charges on HA, which can improve osteogenic response both, *in vitro* and *in vivo*.[85,113] Table 2.1 summarizes the polarization induced *in vitro/ in vivo* response of HA. The polarization enhances cell adhesion/ spreading in comparison to unpolarized HA, where adhered cells had round shapes after 1 h of incubation.[106] Improved osteoblastic activity and promotion of new bone formation have been demonstrated on both, positively and negatively charged surfaces in comparison to uncharged surfaces, coupled with suppressed osteoclast activity on the positively charged surfaces.[102,104,112,183] It has also been reported that the amount of DNA content is higher on negatively charged HA surface in comparison to positively charged as well as uncharged HA surface.[108] In addition, the negatively polarized HA surface exhibits higher osteobonding ability in comparison to positively polarized HA surface.[113,184,185] *In-vivo* implantation of the polarized HA in rabbit femur suggested new bone growth.[112] In addition, the alkaline phosphatise (ALP) depicts positive staining in central region of polarized HA as compared to unpolarized HA after 3 weeks of implantation.[112] Early adsorption of fibrin protein was observed to be accelerated in vicinity of negatively polarized HA implant, in rat tibiae.[186] Fibrin promotes platelets attachment and activation, which

triggers the release of various growth factors that further stimulate cell proliferation, tissue regeneration and new bone formation.[186] The influence of polarized HA is not limited only to bone but also shows significant effects on soft tissues such as, mediating the regeneration of blood vessels and epidermal recovery during the process of wound healing in *in-vivo* models.[187,188] The early mineralisation and apatite layer formation resembling with that of bone has also been observed on negatively charged surface of HA in comparison to unpolarized HA surface. The apatite layer formation on the positively charged HA surface has not been observed, when dipped in simulated body fluid (SBF).[95,107] When proteins, amino acids and various cations/ anions present in SBF/ culture media comes in contact with the polarized surface, they can get repelled/ attracted depending on the surface charge of the substrate. The positive Ca^{2+} cations were adsorbed on negatively charged surface of HA and consequently, promoted cell adhesion.[111] Whereas, anions are attracted towards positively charged HA surface, which do not support mineralisation and thereby, leads to limited cells adhesion.[111] Fig. 2.11 depicts that in contrast to uncharged HA surface, negatively charged HA surface supports apatite nucleation, cell adhesion and proliferation, while negligible effects was observed on positively charged HA surface. It has been reported that, when polarized HA is immersed in SBF, the negatively charged surface of HA facilitates the adsorption of Ca^{2+} ions and thereby, forming Ca-rich amorphous calcium phosphate (ACP). Accumulation of Ca^{2+} ions increases the positive charge on the negatively polarized HA surface, which further attracts the negative PO_4^{3-} ions present in SBF, forming Ca-poor ACP that ultimately crystallizes into bone like apatite.[189] Apart from mineralisation, negatively charged surface of HA also promote osteobonding capacity and new bone formation in contrast to uncharged HA surface, when implanted in dog femur.[113] After 7 days of implantation, the new bone formation on HA surface as well as cortical bone surface escorted by monolayer of osteoblast cells were observed. After 14 days of implantation, a thick layer

of bone formation on negatively polarized surface has been observed and the gap is almost filled after 28 days. In case of unpolarized surface of HA, newly formed bone was surrounded by fibrin, various blood capillaries and fibroblast cells.

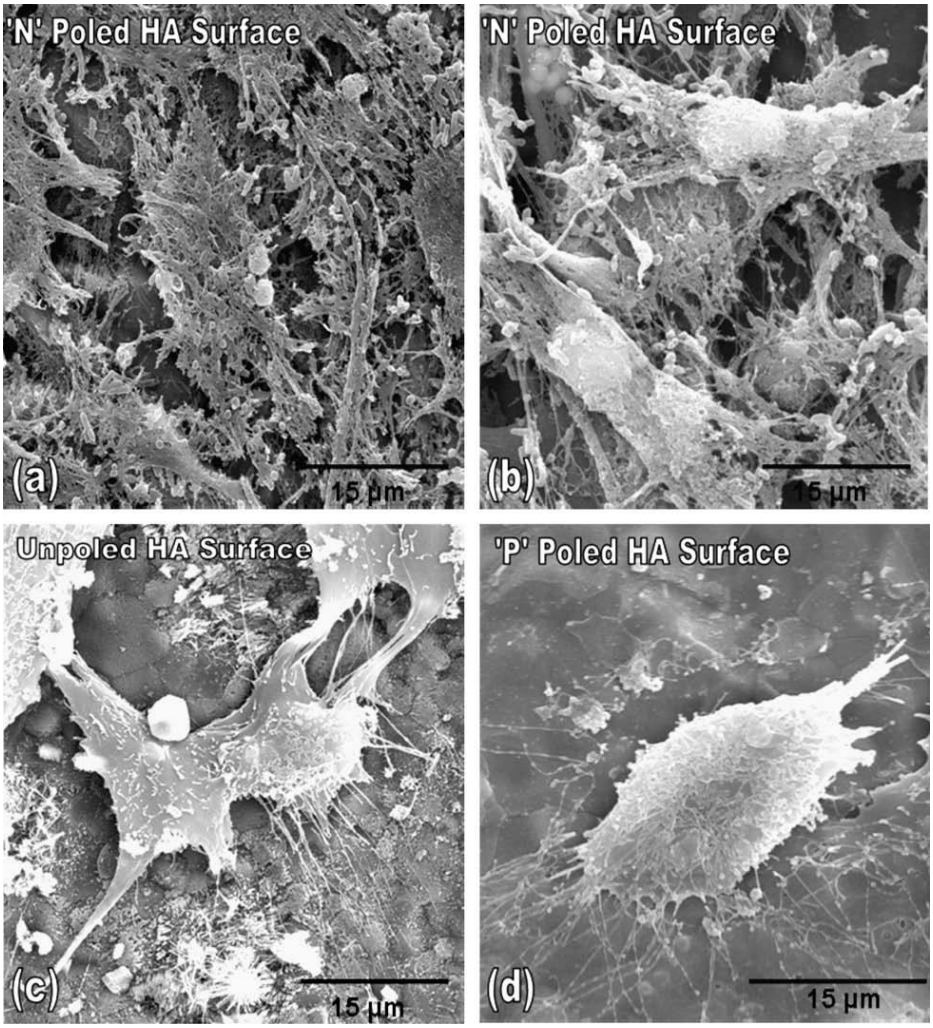

Fig. 2.11: Scanning electron microscopic images demonstrating the functionality of human fetal osteoblast cells on negatively (a, b), unpolarized (c) and positively (d) polarized HA surfaces.[107] (Reproduced with permission from Elsevier)

After 14 days, fibrin layers were deformed, and segmented layers of newly formed bone tissue surrounded by blood capillaries and osteoblastic cells were observed. At the later stage, newly formed bone was in direct contact with unpolarized HA surface, but insufficient to fill the gap. It has also been reported that implantation of polarized HA in calvarial bone defected

mice model, shows the directed bone growth towards positively and negatively charged HA surfaces from the site of injury, which forms bridge.[104] However, un-polarized HA surface does not support any kind of bone bridging and depicts only disjointed bone formation. This unidirectional bone formation can be understood by the fact that during fracture healing, the movement, differentiation and attachment of mesenchymal stem cells (MSC), already present in body, may alter due to differential adsorption of protein on polarized surface.[190,191] In initial phase of implantation, MSC moves towards the implant surface and soon start producing its own extra-cellular matrix, which modifies the implant surface.[190] Later on, MSC start differentiating into osteoblast cells, regulated by transcription factors (Runx2 and osterix).[192] These osteoblast cells secrete essential bone matrix for mineralization, and are interconnected by gap junction to form woven bone.[190] Therefore, *in-vitro* as well as *in-vivo* studies suggest that induced electrical activity in HA significantly improves its biological response over unpolarized HA.

Table 2.1: *In vitro*/ *in vivo* responses of electrically polarised HA

Sr. No.	Polarization conditions	Cell lines/ implantation studies	In vivo/ in vitro Response	Ref.
1	300°C in air under 100 kV/m DC field for 2 h.	MC3T3-E1, L929, SK-N-SH cells	Well spread multilayer of osteoblast cells were observed on N-surface whereas, contracted and inhibited cells proliferation was observed on P-and O-surfaces.	Ohgaki et al. [111]

2	400°C, under 2 kV/cm DC electric field for 1 h.	Human fetal osteoblast cells	More flattened and confluent cell layers were seen on N-surface as compared to O-surface; whereas proliferation was inhibited on P-surface.	Bodhak et al.[107]
3	400°C in air under 5 kV/cm DC electric field for 1 h.	Mesenchymal stem cells, isolated from mouse.	Cells spreading were accelerated (as early as 1 h after incubation) on both N- and P-surfaces in comparison to O-surface.	Nakamura et al.[106]
4	130°C, under 25 kV DC electric field.	SaOS-2 cells	Significant difference was seen between poled and unpoled surfaces in terms of cells proliferation, morphology and attachment.	Baxter et al.[193]
5	300°C, under 1 kV/cm DC field for 1 h.	Implanted in rat tibiae	Fibrin adsorption was enhanced on N- and P-surfaces after 5 min of implantation, which later on induced early osteoconduction.	Nakamura et al.[186]
6	300°C, under 2 kV/cm of DC field	Implanted in rat calvarium	Osteogenesis and new bone formation was accelerated	Teng et al.[184]

	for 1 h.		on N-surface in comparison to O-surface, while on P-surface, negligible or no bone growth was observed.	
7	400°C, under 4 kV/cm DC field for 1 h.	Implanted in rabbit femoral condyle	Osteoconductivity and new bone formation was accelerated on polarized HA.	Ohba et al.[194]
8	400°C, under 5 kV/cm DC field.	MC3T3 cell line	Both positively and negatively polarized HA promote cell spreading and migration towards wound area.	Nakamura et al.[195]
9	300°C, under 1 kV/cm DC field for 1 h.	Implanted in tibial and femoral diaphysis of rabbit	Increased osteobonding ability on N- surface in comparison to other surfaces. Enhanced new bone formation was observed on both N and P-surfaces, leading to complete gap filled after 4 weeks of implantation.	Nakamura et al.[185]
10	DC field of 1 kV/cm for 1 h.	Implanted in femoral and tibial	Accelerated new bone formation in proximity of	Kobayashi et al.[196]

		bone of dog	N- over P- surfaces as well as on O- surface.	

2.4. Human hard tissue as a functionally graded structure

Living bone is a classic example of functionally graded material.[197] Bone is composed of compact part combined with spongy inner section.[198] Spongy section is called the cancellous bone having many pores while the compact bone has negligible pores. The pores in the cancellous bone provide pathway to bone marrow to regulate the blood supply. The living bone changes in composition from inner spongy section to outer dense section, called compact bone.[198,199] This graded structure together provides mechanical flexibility to the bone. Outer dense compact bone provides strength while the stress applied is slowly transferred to the spongy portion which ultimately provides flexibility. Another example of natural graded structure is tendon to bone and cartilage to bone insertions.[200] The tendon to bone insertion is a ligament that provides an interface between two extremely different tissues. While tendon is a soft tissue and bone is a hard tissue. Similar is the case in cartilage to bone insertion. These graded structures are able to withstand variety of mechanical loadings.[201] In the case of long bones, the cross-section of the long bone exhibits structural change from cortical to cancellous bone which is gradual without the presence of abrupt interfaces that further facilitates in smooth variation of mechanical properties. Human teeth are also functionally graded structures.[202] The upper surface of teeth is composed of hydroxyapatite (HA) crystallites as well as hard enamel and the inner section is made of dentine having collagen fibrils along with HA.[202] The upper surface of teeth provides hardness, brittleness and is resistant to wear whereas inner section provides flexibility. This gradual transition from enamel to dentine or dentine to enamel enables the teeth to execute various mechanical functionalities.[203] Another example is human intervertebral disk which is

also a natural graded structure.[199] Similarly, there are many other graded structures in human body varying from cellular to tissue level.

2.4.1. Need for FGMs in prosthetic implants

Generally, materials, used for prosthetic implants in load bearing applications, are stiffer than human bone tissue and therefore there is an uneven distribution of stress upon implantation.[204] When the implant material is placed at a fracture site, the original stress and strain distribution gets altered i.e., the load acting on the bone's trabecular structure and cortex gets shared with the stiffer biomaterial. According to Wolff's law, bone remodels upon external, internal and physiological stress and strain application.[12,13] On placement of stiffer biomaterial these forces are now predominantly concentrated on the implant material and in this process bone observes minimum load which ultimately results in bone resorption. This process is known as stress shielding effect. However, a less stiff biomaterial enhances the shear stress between the implant and surrounding bone tissue which can result in interface motion. In addition, based on the present surgical advancement and the type of implant material utilized, revision surgery becomes common case which is generally troublesome for the patients. In the case of grafts, aseptic loosening is common due to bone resorption as well as wear particles released from the prosthetic implant material which creates inflammatory response. Therefore, a critical choice of material is very necessary. Considering the complexity of stress and strain pattern existing in living bone, functionally graded materials (FGM) are an appropriate alternative as their properties can be adjusted according to the desired application. In addition, implants consisting of conventional materials (monolithic structure) and composites (heterogeneous structure) are often inappropriate due to the presence of abrupt interfaces, which often results in interfacial failure. FGMs are generally composite materials in which properties such as grain size, texturization level, density, microstructure and composition gradually change in more than one spatial direction

according to the application. FGMs eliminate the macroscopic boundaries within material, which results in continuous change in mechanical, physical as well as biochemical properties.[205]

FGM is composed of two or more different materials or constituent phases with each material/phase are designated as 'material ingradient'.[199] In FGM, each material/phase varies gradually in composition resulting in smooth variation of properties such as density, texture, microstructure, thermal expansion coefficient, thermal conductivity, etc.[199,206] The gradual variation of the above mentioned properties is essential for maintaining the desired property, for e.g., if there is a sudden change in the thermal expansion coefficient at the interface, residual thermal stresses would be developed at high temperature which leads to the development of crack and finally degradation of mechanical properties.[199,206,207] Therefore, the graded interface in the FGM provides smooth transfer of thermal stress resulting in superior mechanical properties.[199,206,207]

In general, FGMs possesses two classic features which make them as an excellent substitute to orthopaedic implants. Firstly, the gradual gradation in the composition and microstructure across the whole volume can provide the bone mimicking response and simultaneously minimizes the consequences of stress shielding effect.[199] Secondly, they possess superior mechanical properties compared to monolithic as well as composite structures. Previously, FGMs are developed having at least one ingredient as a metallic phase. These FGMs of metal and metal-polymer based compositions causes continued osteointegration, generates debris/microscopic particulates on friction between articulating surfaces of implants, degradation of the implant, bone resorption, etc.[206,207] Due to these disadvantages, functionally graded ceramics (FGCs) have gained significant attention because of their endurance to be operative at severe conditions of temperature, corrosive environment, abrasion, large mechanical loadings as well as thermal-induced stresses.[206] In addition to

these properties ceramics can potentially mimick the electro-active response of natural bone. Overall, owing to the inherent nature of bone as an electrically active tissue as well as having a functionally graded structure, the development of electro-active FGMs can be anticipated to provide better functional response as far as the integration of implant with the host bone tissue and its survival period is concerned.[130]

Synthetic HA has been always an excellent choice for the orthopaedic implant material but however, due to its poor mechanical and electrical properties, it is inadequate for the mechano-electrically bone implants material. Therefore, piezocomposites have been developed utilizing $BaTiO_3$ (BT) as reinforcement phase in the HA matrix.[171,208] BT is a well-known piezoelectric as well as ferroelectric material. In addition, BT has been demonstrated to be a biocompatible material both *in-vitro* and *in-vivo*.[9,209,210] Further, it is reported that the addition of BT as a secondary phase improves the mechanical properties of various composite systems.[171,208] Therefore, piezocomposite of HA with varying amounts of BT (0, 20, 40, 60, 80 and 100 wt %) were developed via multistage spark plasma sintering (SPS) route.[208] Out of these piezocomposites, HA-40 wt % BT has been reported to have mechanical (compressive strength, elastic modulus) as well as electrical (dielectric, Ac conductivity and piezoelectric strain coefficient) properties similar with that of the natural bone.[208] Thereafter, in followed study, the piezocomposites of HA-20BT and HA-40BT were electrically polarized (10 kV/cm).[211] These polarized composites demonstrated enhanced cytocompatibilty towards mouse fibroblasts L929 and osteogenic cells under the pulsed E-field (0.5 - 4 V/cm, 400 μs) stimulation in *in-vitro*.[211] In further study, dense piezocomposite of HA-xBT (x = 25, 40, 60, 75) were developed using single stage SPS route.[212] These composites successfully retains OH^- ions in HA phase as demonstrated through FTIR as well as thermal characterization techniques. Also, enhanced dielectric and pyroelectric properties were achieved along with controlled ferroelectric phase content.[212]

Considering these developments, alkali niobate ceramic such as ferroelectric $N_{0.5}K_{0.5}NbO_3$ has been an excellent alternative due to its high piezoelectric strain coefficient: d_{33} ~ 260 pC/N, high curie temperature: T_C ~ 420°C, electromechanical coupling coefficient: k_p ~ 0.48, mechanical quality factor: Q_m ~ 280 and dielectric constant: ε ~ 657 as well as its relatively lower density (~ 4.51 gm/cm^3) as compared with other piezoelectric biomaterials.[213,214,215,216,217] In addition, ferroelectric NKN ($Na_xK_yNbO_3$; $0 \leq x \leq 0.8$, $0.2 \leq y \leq 1$) is a patented biocompatible orthopaedic implant material because of its excellent viability towards human monocytes.[218] In this respect, FGM comprising of HA with NKN interlayers were developed via SPS route.[130] The advantage of developing HA based FGM is that the excellent bioactive nature of HA is not compromised while the increased dielectric and AC conductivity properties were achieved along with reasonable piezoelectric strain coefficient (4.2 pC N^{-1}).[130] In addition, cell adhesion as well as enhanced cell proliferation of human osteoblast-like SaOS2 cells on the developed FGM was achieved.[130] In another report, FGM of HA with LNKN ($Li_x(Na_{0.5}K_{0.5})_{1-x}NbO_3$; x ~ 0.06) interlayer were developed via tape casting route.[219] In LNKN, Li substitutes at A-site in NKN perovskite structure which further enhances the polarizability of NKN. The developed laminated composite / FGM of LNKN has been reported to increase the polarizability of HA by 6-times.[219] The developed laminated composite also has reasonable piezoelectric strain coefficient (d_{33} ~ 2 pC N^{-1}), comparable with that of the natural bone.[219] In addition, when immersed in simulated body fluid (SBF) for 3, 7 and 14 days, increased growth of mineral apatite was observed on the developed FGM. In this view, the developed FGM of LNKN can be suggested as a potential substitute for electroactive prosthetic implants.[219]

2.5. Summary

Owing to the remarkable electrical response of living bone and their consequences in various bone metabolic activities, the need for the development of electro-active prosthetic implant can be realized. Many materials have been developed based on their biocompatibility and bone mimicking response. Among these, hydroxyapatite (HA) has been an excellent choice because of its structural, chemical and morphological similarity with the bone mineral apatite. In addition, the ability of synthetic HA to convert to an electret under low polarizing field ($\leq$ 1 kV/cm) is an essential measure to utilize it as an electro-active prosthetic implant material. These HA electrets have displayed excellent osteointegration with the bone cells. It is well-explored that properly tuned E-field also enhances the cell material interaction. Therefore, the need to develop an understanding on the interaction of E-field with a single cell is required. This would facilitate the selection of properly tuned E-field parameter to further enhance the cell-material interaction. In addition, HA electrets as well as their usability to develop functionally graded materials along with the other electroactive bioceramics would further fill the gap for a better bone mimicking material having excellent biocompatibility as well as electrical, mechanical, structural and morphological characteristics similar to that bone.

References

[1] JO Hollinger, TA Einhorn, BA Doll and C Steir, 'Bone Tissue Engineering', CRC Press LLC, 2005.

[2] FR Baxter, CR Bowen, IG Turner and ACE Dent, "Electrically active bioceramics: A review of interfacial responses", *Annals of Biomedical Engineering*, (2010), 38(6), 2079-2092.

[3] M S-Shojai, M-T. Khorasani, E. D.-Khoshdargi and A. Jamshidi, "Synthesis methods for nanosized hydroxyapatite with diverse structures", *Acta Biomaterialia*, 9(8), (2013), 7591-7621.

[4] MA Meyers, PY Chen, AYM Lin and Y Seki, "Biological materials: Structure and mechanical properties", *Progress Materials Science*, 53, (2008), 1-206.

[5] JC Wall, SK Chatterji and JW Jeffery, "The influence that bone density and the orientation and particle size of the mineral phase have on the mechanical properties of bone", *Journal of Bioengineering*, 2(6),(1978), 517-526.

[6] DB Burr, "The contribution of the organic matrix to bone's material properties", *Bone*, 31(1), (2002), 8-11.

[7] SM Bowman, J Zeind, LJ Gibson, WC Hayes and TA McMahon, "The tensile behavior of demineralized bovine cortical bone", *Journal of Biomechanics*, 29(11), (1996), 1497-1501.

[8] W.S.S. Jee, Integrated bone tissue physiology: anatomy and physiology. In: Bone Mechanics Handbook, edited by S. C. Cowin. Boca Raton: CRC Press, 2001.

[9] J.B. Park, A. F. von Recum, G. H. Kenner, B. J. Kelly, W. W. Coffeen, and M. F. Grether, "Piezoelectric ceramic implants: a feasibility study" *Journal of Biomedical Materials Research*, 14(3): (1980), 269-277.

[10] C. H. Turner, "Three rules for bone adaptation to mechanical stimuli" *Bone* 23(5): (1988), 399-407.

[11] P. J. Nijweide, E. H. Burger, J. K. Nulend, and A. Van der Plas, “The osteocyte. In: Principles of Bone Biology”, edited by J. Bilezikian, Z. Raiz, and T. J. Martin. London: Academic Press, 1996

[12] J. D. Wolff, Der gesetz der transformation der knochen. Berlin: A. Hirschwald, 1892.

[13] B.M. Isaacson and R.D. Bloebaum, “Bone bioelectricity: What have we learned in the past 160 years?”, *Journal of Biomedical Materials Research Part A*, 95A: (2010) 1270-1279.

[14] R. Nuccitelli, "A role for endogenous electric fields in wound healing." *Current topics in developmental biology* 58.2 (2003): 1-26.

[15] R.H.W Funk, “Endogenous electric fields as guiding cue for cell migration”, *Frontiers in physiology* 6 (2015): 143.

[16] KR Robinson, “The responses of cells to electrical fields: A review”, *Journal of Cell Biology*, 101: (1985), 2023-2027.

[17] K. H. Schoenbach, E. Neumann, R. Heller, P. T. Vernier, J. Teissie and S.J. Beebe, Introduction, in Bioelectrics, H. Akiyama and R. Heller (eds.), Springer Japan, Tokyo, 2017, 1-40.

[18] DT Reilly and AH Burstein, “The mechanical properties of cortical bone”, *The Journal of Bone and Joint Surgery*, 56A: (1974), 1001-1022.

[19] J. Sela, UM Gross, D. Kohavi, J. Shani, DD Dean, BD Boyan and Z. Schwartz, “Primary mineralization at the surfaces of implants”, *Critical reviews in oral biology and medicine : an official publication of the American Association of Oral Biologists*, 11: (2000), 423-436.

[20] E. Fukada, and I. Yasuda, “On the piezoelectric effect of bone”, *Journal of the Physical Society of Japan*, 12(10): (1957), 1158-1162.

[21] J. Curie, and P. Curie, "Développement par compression de l'électricité polaire dans les cristaux hémièdres à faces inclinées." *Bulletin de minéralogie* 3.4 (1880): 90-93.

[22] I. Yasuda, H. Nagayama, T. Kato, O. Hara, K. Okada, K. Noguchi, and T. Sata, "Fundamental problems in the treatment of fracture," *Journal of the Kyoto Medical Society*, 4,(1953), 395-4(in Japanese).

[23] E. Fukada, and I. Yasuda, "Piezoelectric effects in collagen", *Japanese Journal of Applied Physics* 3(2): (1964), 117-121.

[24] S.B. Lang, "Pyroelectric effect in bone and tendon", *Nature*, 212, (1966), 704-705.

[25] S.B. Lang, "Pyroelectricity: Occurrence in biological materials and possible physiological implications", *Ferroelectrics*, 34, (1981), 3-9.

[26] N. Guzelsu and W.R. Walsh, "Streaming potential of intact wet bone", *Journal of Biomechanics*, 23, (1990), 673-685.

[27] M.A. El Messiery, G.W. Hastings and S. Rakowski, "Ferro-electricity of dry cortical bone", *Journal of Biomedical Engineering*, 1, (1979), 63-65.

[28] S. Mascarenhas, "The electret effect in bone and biopolymers and the bound-water problem", *Annals of the New York Academy of Sciences*, 238: (1974), 36-52.

[29] S. Itoh and K. Yamashita, "Electrical Properties of Human Bone as an Electret", *Phosphorus Research Bulletin*, 35: (2019), 38-41

[30] M. Braden, A.G. Bairstow, I. Beider and B.G. Ritter, "Electrical and piezo-electrical properties of dental hard tissues", *Nature* 212, (1966), 1565-1566.

[31] S. Sarah, C. Li, Y.J. Choi, L. Michael and L.K. David, "Bioelectric modulation of wound healing in a 3D in vitro model of tissue engineered bone", *Biomaterials* 34, (2013), 6695-6705.

[32] A.A. Marino, R.O. Becker and S.C. Soderholm, "Origin of the piezoelectric effect in bone", *Calcified Tissue Research* 8**,** (1977), 177-180.

[33] GW Hastings and FA Mahmud, "Electrical effects in bone", *Journal of Biomedical Engneering*, 10, (1988), 515-521.

[34] MI Kay, RA Young and AS Posner, “Crystal structure of hydroxyapatite”, *Nature*, 204, (1964), 1050.

[35] CAL Bassett and RO Becker, “Generation of electric potentials by bone in response to mechanical stress”, *Science*, 137, (1962), 106369.

[36] ZB Friendenberg, R Dyer and CT Brighton, “Electroosteograms of long bones of immature rabbits”, *Journal of Dental Research*, 50, (1971), 635-639.

[37] G. W Hastings and F. A. Mahmud, “The electromechanical properties of fluid-filled bone: a new dimension”, *Journal of Materials Science: Materials in Medicine* 2(2), (1991), 118-124.

[38] H. Maeda, K. Tsuda and E. Fukada, “The dependence on temperature and hydration of piezoelectric, dielectric and elastic constants of bone”, *Japanese Journal of Applied Physics*, 15(12): (1976), 2333–2336.

[39] GW Hastings, MA El Messiery and S Rakowski, “Mechanoelectrical properties of bone”, *Biomaterials*, 2, (1981), 225-233.

[40] W F. Boron and B. L. Emile, "A Medical Physiology: A Cellular and Molecular Approach", ISBN: 978-1-4377-1753-2, 2012.

[41] E. R. Kandel, J.H. Schwartz, T.M. Jessel, S.A. Siegelbaum and A.J. Hudspeth, “Principles of Neural Science”, Fifth Edition, Mcgraw Hill,2013, ISBN:978-0-07-181001-2

[42] R. Nuccitelli, “Endogenous electric fields in embryos during development, regeneration and wound healing”, *Radiation Protection Dosimetry,* 106 (4), (2003), 375-383.

[43] D. M. Colin and M. Zhao, “Physiological electrical fields modify cell behaviour”, *Bio Essays*, 19 (9), (2005), 819-826.

[44] F. Fröhlich and D. A. McCormick, “Endogenous Electric Fields May Guide Neocortical Network Activity”, *Neuron*, 67 (1), (2010), 129-143.

[45] E. Neumann, M. Schaefer-Ridder, Y. Wang and P.H. Hofschneider, "Gene transfer into mouse lyoma cells by electroporation in high electric fields", *The EMBO journal,* 1 (7), (1982), 841-845.

[46] A.K. Dubey, K. Balani and B. Basu, in *Nanomedicine: Technologies and Applications*, ed. T.J.Webster, Woodhead Publishing, Cambridge, 1st edn, 2012, ch.18, pp. 537-570.

[47] M. L. Yarmush, A. Golberg, G. Serša, T. Kotnik and D. Miklavčič, "Electroporation-Based Technologies for Medicines: Principles, Applications, and Challenges", *Annual Reviews in Biomedical Engineering,* 16 (1), (2014), 295-320.

[48] T. Batista Napotnik and D. Miklavčič, "In vitro electroporation detection method - An Overview", *Bioelectrochemistry,* 120, (2018), 166-182.

[49] K. H. Schoenbach, S. Katsuki, R. H. Stark, E. S. Buescher and S. J. Beebe, "Bioelectrics - New application for pulsed power technology", *IEEE Transactions in Plasma Science,* 30(1), (2002), 293-300.

[50] T. Batista Napotnik, M. Reberšek, P. T. Vernier, B. Mali, and D. Miklavčič, "Effects of high voltage nanosecond electric pulses on eukaryotic cells (*in vitro*): A systematic review", *Bioelectrochemistry,* 110, (2016), 1-12.

[51] K. H. Schoenbach, S. J. Beebe and E. S. Buescher, "Intracellular effect of ultrashort electrical pulses", *Bioelectromagnetics,* 22 (6), (2001), 440-448.

[52] K. R. Robinson, "The responses of cells to electrical fields: a review.", *Journal of Cell Biology,* 101 (6), (1985), 2023-2027.

[53] T.Y. Tsong, "Electroporation of cell membranes", *Biophysical Journal,* 60 (2), (1991), 297-306.

[54] S. J. Beebe, P. M. Fox, P. M, L. J. Rec, K. Somers, R. H. Stark and K. H. Schoenbach, "Nanosecond pulsed electric field (nsPEF) effects on cells and tissues: Apoptosis induction

and tumor growth inhibition", *IEEE Transactions in Plasma Science,* 30 (1), (2002), 286-292.

[55] U. Zimmermann and J. Vienken, "Electric field-induced cell-to-cell fusion", *The Journal of Membrane Biology,* 67 (1), (1982), 165-182.

[56] T.-K. Wong and E. Neumann, "Electric field mediated gene transfer", *Biochemical and Biophysical Research Communications,* 107 (2), (1982), 584-587.

[57] S. J. Beebe, "Bioelectrics in Basic Science and Medicine: Impact of Electric Fields on Cellular Structures and Functions", *Journal of Nanomedicine and Nanotechnology*, 4(2), (2013), 1-8.

[58] T. R. Gowrishankar and J. C. Weaver, "An approach to electrical modeling of single and multiple cells", *Proceedings of the National Academy of Sciences in the United States of America*, 100 (6), (2003), 3203-3208.

[59] J. Ferrier, SM Ross, J. Kanehisa and JE Aubin, "Osteoclasts and osteoblasts migrate in opposite directions in response to a constant electrical field.", *Journal of Cellular Physiology*, 129: (1986), 283–288.

[60] HK Soong, WC Parkinson, S Bafna, GL Sulik and SC Huang, "Movements of cultured corneal epithelial cells and stromal fibroblasts in electric fields.", *Investigative Ophthalmology and Visual Science*, 31: (1990), 2278-2282.

[61] LA Norton, GA Rodan and LA Bourret, "Epiphyseal cartilage cAMP changes produced by electrical and mechanical perturbations." *Clinical Orthopaedics and Related Research*, 124: (1977), 59–68

[62] T. Albrektsson and C. Johansson, "Osteoinduction, osteoconduction and osseointegration.", *European Spine Journal*, 10 (Suppl 2): (2001), S96–S101.

[63] K. H. Schoenbach, F. E. Peterkin, R. W. Alden and S. J. Beebe, "The effect of pulsed electric fields on biological cells: experiments and applications", *IEEE Transactions in Plasma Science*, 25 (2), (1997), 284-292.

[64] J. Deng, K. H. Schoenbach, E. S. Buescher, P. S. Hair, P. M. Fox and S. J. Beebe, "The Effects of Intense Submicrosecond Electrical Pulses on Cells", *Biophysical Journal,* 2003, 84 (4), (2003), 2709-2714.

[65] A. K. Dubey, S. Dutta-Gupta, R. Kumar, A. Tewari and B. Basu, "Time constant determination for electrical equivalent of biological cells", *Journal of Applied Physics,* 105(8), (2009), 084705.

[66] A. K. Dubey, M. Banerjee and B. Basu, **"**Biological cell–electrical field interaction: stochastic approach", *Journal of Biological Physics,* 37 (1), (2011), 39-50.

[67] A. K. Dubey, R. Kumar, M. Banerjee and B. Basu, "Analytical Computation of Electric Field for Onset of Electroporation", *Journal of Computational and Theoretical Nanoscience,* 9 (1), (2012), 137-143.

[68] P. Ellappan and R. Sundararajan, "A simulation study of the electrical model of a biological cell." *Journal of Electrostatics,* 63 (3), (2005), 297-307.

[69] SR Leadley, MC Davies, CC Ribeiro, MA Barbosa, AJ Paul and JF Watts, "Investigation of the dissolution of the bioceramic hydroxyapatite in the presence of titanium ions using TOF-SIMS and XPS", *Biomaterials*, 18, (1997), 311-316.

[70] L. L. Hench, "Bioceramics: From Concept to Clinic*", Journal of the American Ceramic Society*, 74, (1991), 1487-1510.

[71] H. B. Lu, C. T. Campbell, D. J. Graham and B. D. Ratner, "Surface Characterization of Hydroxyapatite and Related Calcium Phosphates by XPS and TOF-SIMS", *Analytical Chemistry*, 72 (13), (2000), 2886-2894.

[72] W. F. de Jong, "The mineral components of bones", *Recueil des Travaux Chimiques des Pays-Bas et de la Belgique*, 45, (1926), 445-448.

[73] R. Z. LeGeros, "Apatites in biological systems", *Progress in Crystal Growth and Characterization*, 4 (1–2), (1981), 1-45.

[74] J. L. Drummond, In Biomaterials in reconstructive surgery, Rubin, L. R., Ed.; The C. V. Mosby Co.: St. Louis, MO, (1983), 103-108.

[75] Garcia R, Doremus RH, 'Electron microscopy of the bone implant interface from a human dental implant' *Journal of Materials Science: Materials in Medicine*, 3, (1992), 154-156.

[76] IS Lee, C Whang, H Kim, J Park, JH Song and S Kim, "Various Ca/P ratios of thin calcium phosphate films", *Materials Science and Engineering C*, 22, (2002), 15-20.

[77] C. Lavernia and J.M. Schoenung, "Calcium-phosphate ceramics as bone substitutes", *American Ceramic Society Bulletin*, 70, (1991), 95-100.

[78] H. W. Kim, J. C. Knowles, H. E. Kim, "Hydroxyapatite/poly(ε-caprolactone) composite coatings on hydroxyapatite porous bone scaffold for drug delivery", *Biomaterials*, 25 (7-8), (2004), 1279-1287.

[79] F. Chiatti, M. D. Piane, P. Ugliengo, and M. Corno, "Water at hydroxyapatite surfaces: the effect of coverage and surface termination as investigated by all-electron B3LYP-D simulations", *Theoretical Chemistry Accounts*, 135(3), (2016), 54.

[80] L. J. Cummings, M. A. Snyder and K. Brisack, Chapter 24 Protein Chromatography on Hydroxyapatite Columns, Editor(s): Richard R. Burgess, Murray P. Deutscher, Methods in Enzymology, Academic Press, 463, (2009), 387-404.

[81] S. Ezhaveni, R. Yuvakkumar, M. Rajkumar, N. M. Sundaram and V. Rajendran, "Preparation and Characterization of Nano-Hydroxyapatite Nanomaterials for Liver Cancer Cell Treatment", *Journal of Nanoscience and Nanotechnology*, 13(3), (2013), 1631-1638.

[82] Guobin Ma and Xiang Yang Liu, "Hydroxyapatite: Hexagonal or Monoclinic?", *Crystal Growth & Design*, 9 (7), (2009), 2991-2994.

[83] M.I. Kay, R.A. Young and A.S. Posner, "Crystal Structure of Hydroxyapatite", *Nature*, 204, (1964), 1050-1052.

[84] J. C. Elliott, P. E. Mackie and R. A. Young, "Monoclinic Hydroxyapatite", *Science*, 180(4090), (1973), 1055-1057.

[85] S. Hu, F. Jia, C. Marinescu, F. Cimpoesu, Y. Qi, Y. Tao, A. Stroppaand and W. Ren, "Ferroelectric polarization of hydroxyapatite from density functional theory", *RSC Advances*, 7 (35), (2017), 21375-21379.

[86] R. A. Young and W. E. Brown, In Biological Mineralization and Demineralization; G. H Nancollas, Ed. Dahlem Konferenzen: Berlin, 1982; pp 101-141.

[87] D. Haverty, and S. A. M. Tofail, K. T. Stanton, and J. B.McMonagle, "Structure and stability of hydroxyapatite: Density functional calculation and Rietveld analysis", *Physical Review B*, 71 (9), (2005), 094103.

[88] J. C. Elliott and R.A. Young, "Conversion of Single Crystals of Chlorapatite into Single Crystals of Hydroxyapatite", *Nature*, 214, (1967), 904-906.

[89] T. Ikoma, A. Yamazaki, S. Nakamura, M. Akao, "Preparation and Structure Refinement of Monoclinic Hydroxyapatite", *Journal of Solid State Chemistry*, 144 (2), (1999), 272-276.

[90] Y. Suetsugu and J. Tanaka, Crystal growth and structure analysis of twin-free monoclinic hydroxyapatite, *Journal of Materials Science: Materials in Medicine*, 13, (8), (2002), 767-772.

[91] N. Horiuchi, M. Nakamura, A. Nagai, K. Katayama and K. Yamashita, "Proton conduction related electrical dipole and space charge polarization in hydroxyapatite", *Journal of Applied Physics*, 112, (2012), 074901.

[92] H. B. V. Rees, M. Mengeot and E. Kostiner, "Monoclinic-hexagonal transition in hydroxyapatite and deuterohydroxyapatite single crystals", *Materials Research Bulletin*, 8 (11), (1973), 1307-1309.

[93] H. Suda, M. Yashima, M. Kakihana and M. Yoshimura, "Monoclinic .tautm. Hexagonal Phase Transition in Hydroxyapatite studied by X-ray Powder Diffraction and Differential Scanning Calorimeter Techniques", *The Journal of Physical Chemistry*, 99, 17, (1995), 6752-6754.

[94] H. Takahashi, M. Yashima, M. Kakihana and M. Yoshimura, "A differential scanning calorimeter study of the monoclinic ($P2_1/b$)↔hexagonal ($P6_3/m$) reversible phase transition in hydroxyapatite", *Thermochimica Acta*, 371 (1-2), (2001), 53-56.

[95] K. Yamashita, N. Oikawa and T. Umegaki, "Acceleration and Deceleration of Bone-Like Crystal Growth on Ceramic Hydroxyapatite by Electric Poling", *Chemistry of Materials* 8(12), (1996), 2697-2700.

[96] S. Nakamura, H. Takeda and K. Yamashita, "Proton transport polarization and depolarization of Hydroxyapatite ceramics", *Journal of Applied Physics*, 89, (2001), 5386-5392.

[97] S. Ramakrishna, J. Mayer, E. Wintermantel and K.W. Leong, "Biomedical application of polymer composite materials: A review", *Composites Science and Technology*, 61, (2001), 1189-1224.

[98] S. Mascarenhas, "The Electret Effect in Bone and Biopolymers and the Bound Water problem", *Annals of the New York Academy of Sciences*, 238, (1974), 36-52.

[99] C. A. L. Bassett, and R. O. Becker, "Generation of Electric Potentials by Bone in Response to Mechanical Stress", 137(3535), (1962), 1063 - 1064.

[100] C. A. L. Bassett, R. J. Pawluk and R. O. Becker, "Electrical currents on bone in vivo", *Nature*, 204, (1964), 652-654.

[101] S. Nakamura, T. Kobayashi, M. Nakamura and K. Yamashita, "Enhanced in vivo responses of osteoblasts in electrostatically activated zones by hydroxyapatite electrets", *Journal of Materials Science: Materials in Medicine*, 20, (2009), 99-103.

[102] S. Nakamura, T. Kobayashi, and K. Yamashita, "Extended bioactivity in the proximity of hydroxyapatite ceramic surfaces induced by polarization charges", *Journal of Biomedical Materials Research* 61, (2002), 593-599.

[103] S. Itoh, S. Nakamura, M. Nakamura, K. Shinomiya, and K. Yamashita, "Enhanced bone ingrowth into hydroxyapatite with interconnected pores by Electrical Polarization", *Biomaterials* 27, (2006), 5572-5579.

[104] S. Itoh, S. Nakamura, T. Kobayashi, K. Shinomiya, K. Yamashita and S. Itoh, S, "Effect of electrical polarization of hydroxyapatite ceramics on new bone formation", *Calcified Tissue International* 78, (2006), 133-142.

[105] S. Itoh S., S. Nakamura, M. Nakamura, K. Shinomiya and K. Yamashita, "Enhanced bone regeneration by electrical polarization of hydroxyapatite", *Artificial Organs* 30, (2006), 863-869.

[106] M. Nakamura, A. Nagai, T. Hentunen, J. Salonen, Y. Sekijima, T. Okura, K. Hashimoto, Y. Toda, H. Monma and K. Yamashita, "Surface electric fields increase osteoblast adhesion through improved wettability on hydroxyapatite electret", *ACS Applied Materials and Interfaces* 1(10), (2009), 2181-2189.

[107] S. Bodhak, S. Bose, and A. Bandyopadhyay, "Role of surface charge and wettability on early stage mineralization and bone cell–materials interactions of polarized hydroxyapatite", *Acta Biomaterialia*, 5, (2009), 2178-2188.

[108] D. Kumar, J. P. Gittings, I.G. Turner, C.R. Bowen, A. Bastida-Hidalgo, and S.H. Cartmell, "Polarization of hydroxyapatite: influence on osteoblast cell proliferation", *Acta Biomaterialia* 6, (2010), 1549-1554.

[109] S. Bodhak, S. Bose and A. Bandyopadhyay, "Electrically polarized HAp-coated Ti: in vitro bone cell-material interactions", *Acta Biomaterialia*, 6, (2010), 641-651.

[110] S. Bodhak, S. Bose and A. Bandyopadhyay, "Bone cell–material interactions on metal-ion doped polarized hydroxyapatite", *Materials Science and Engineering C*, 31, (2011), 755-761.

[111] M. Ohgaki, T. Kizuki, M. Katsura and K. Yamashita, "Manipulation of selective cell adhesion and growth by surface charges of electrically polarized hydroxyapatite", *Journal of Biomedical Materials Research*, 57, (2001), 366-373.

[112] S. Itoh, S. Nakamura, M. Nakamura, K. Shinomiya, K. Yamashita, "Enhanced bone ingrowth into hydroxyapatite with interconnected pores by Electrical Polarization", *Biomaterials*, 27 (32), (2006), 5572-5579.

[113] T. Kobayashi, S. Nakamura, K. Yamashita, "Enhanced osteobonding by negative surface charges of electrically polarized hydroxyapatite", *Journal of Biomedical Materials Research*, 57, (2001), 477-484.

[114] A. Nagai, K. Yamashita, M. Imamura, H. Azuma, "Hydroxyapatite electret accelerates reendothelialization and attenuates intimal hyperplasia occurring after endothelial removal of the rabbit carotid artery", *Life Sciences*, 82 (23–24), (2008), 1162-1168.

[115] R. Okabayashi, M. Nakamura, T. Okabayashi, Y. Tanaka, A. Nagai and K. Yamashita, "Efficacy of polarized hydroxyapatite and silk fibroin composite dressing gel on epidermal recovery from full-thickness skin wounds", *Journal of Biomedical Materials Research Part B*, 90 B, (2009), 641-646.

[116] N. Hitmi, C. LaCabanne, R.A. Young, "OH^- dipole reorientability in hydroxyapatites: Effect of tunnel size", *Journal of Physics and Chemistry of Solids*, 47 (6), (1986), 533-546.

[117] K. Yamashita, K. Kitagaki, and T. Umegaki, "Thermal Instability and Proton Conductivity of Ceramic Hydroxyapatite at High Temperatures", *Journal of the American Ceramic Society*, 78, (1995), 1191-1197.

[118] G. C. Maiti and F. Friedemann, "Influence of fluorine substitution on the proton conductivity of hydroxyapatite", *Journal of the Chemical Society, Dalton Transactions*, 0, (1981), 949-955.

[119] M. Yashima, Y. Yonehara, and H. Fujimori, "Experimental Visualization of Chemical Bonding and Structural Disorder in Hydroxyapatite through Charge and Nuclear-Density Analysis", *The Journal of Physical Chemistry C*, 115 (50), (2011), 25077-25087.

[120] N. Horiuchi, N. Wada, K. Nozaki, M. Nakamura, A. Nagai and K. Yamashita, "Dielectric relaxation in monoclinic hydroxyapatite: Observation of hydroxide ion dipoles", *Journal of Applied Physics*, 119, (8), (2016), 084903.

[121] N. Horiuchi, K. Madokoro, K. Nozaki, M. Nakamura, K. Katayama, A. Nagai and K. Yamashita, "Electrical conductivity of polycrystalline hydroxyapatite and its application to electret formation", *Solid State Ionics*, 315, (2018), 19-25.

[122] C. Bucci, R. Fieschiand and G. Guidi, "Ionic Thermocurrents in Dielectrics", *Physical Review Letters*, 148, (1966), 816.

[123] M. Davies, P. J. Hains, and G. Williams, "Molecular motion in the supercooled liquid state: ion pairs in slow motion", *Journal of Chemical Society Faraday Transactions 2: Molecular and Chemical Physics*, 69, (1973), 1785-1792.

[124] Vanderschueren J., Gasiot J. (1979) Field-induced thermally stimulated currents. In: Bräunlich P. (eds) Thermally Stimulated Relaxation in Solids. Topics in Applied Physics, vol 37. Springer, Berlin, Heidelberg.

[125] A. K. Dubey, H. Yamada and K. Kakimoto, "Space charge polarization induced augmented in vitro bioactivity of piezoelectric (Na, K) NbO_3", *Journal of Applied Physics*, 114, (2013), 124701.

[126] G.M. Sessler, 1980, "Electrets," in Field-Induced Thermally Stimulated Currents, Springer-Verlag, Berlin, Ch. 4.

[127] L.I. Grossweiner, "A Note on the Analysis of First-Order Glow Curves", *Journal of Applied Physics*, 24(10), (1953), 1306.

[128] M. Nagai and T. Nishino, "Surface conduction of porous hydroxyapatite ceramics at elevated temperatures", *Solid State Ionics*, 28–30, 2, (1988), 1456-1461.

[129] J.P. Gittings, C.R. Bowen, A.C.E. Dent, I.G. Turner, F.R. Baxter and J.B. Chaudhuri, "Electrical characterization of hydroxyapatite-based bioceramics", *Acta Biomaterialia*, 5(2), (2009), 743-754.

[130] A. K. Dubey, K. Kakimoto, A. Obata and T. Kasuga, "Enhanced polarization of hydroxyapatite using the design concept of functionally graded materials with sodium potassium niobate", *RSC Advances*, 4 (47), (2014), 24601-24611.

[131] S. Kasamatsu and O. Sugino, "First-principles investigation of polarization and ion conduction mechanisms in hydroxyapatite", *Physical Chemistry Chemical Physics*, 20(13), (2018), 8744-8752.

[132] T. Takahashi, S. Tanase and O. Yamamoto, "Electrical conductivity of some hydroxyapatites", *Electrochimica Acta*, 23(4), (1978), 369-373.

[133] K. Yamashita, H. Owada, T. Umegaki, T. Kanazawa and T. Futagami, "Ionic conduction in apatite solid solutions", *Solid State Ionics*, 28–30, (1), (1988), 660-663.

[134] K. Yamashita, "Electrically Active Materials for Medical Devices", Ch. 7, 91-102 (2016).

[135] K. Matsunaga and A. Kuwabara, "First-principles study of vacancy formation in hydroxyapatite", *Physical Review B*, 75 (1), (2007), 014102.

[136] Y. Tanaka, M. Nakamura, A. Nagai, T. Toyama and K. Yamashita, "Ionic conduction mechanism in Ca-deficient hydroxyapatite whiskers", *Materials Science and Engineering. B*, 161 (1-3), (2009), 115-119.

[137] S.A.M. Tofail, C. Baldisseri, D. Haverty, J.B. McMonagle, and J. Erhart, "Pyroelectric surface charge in hydroxyapatite ceramics", *Journal of Applied Physics*, 106, (2009), 106104.

[138] H. Fujimori, H. Toya, K. Ioku, S. Goto and M. Yoshimura, "In situ observation of defects in hydroxyapatite up to 1200°C by ultraviolet Raman spectroscopy", *Chemical Physics Letters* 325(4),(2000), 383-388.

[139] N. Hitmi, D. Chatain, C. Lacabanne, J. Dugas, J.C. Trombe, C. Rey and G. Montel, "TSC study of dipolar reorientations in hydroxyapatites", *Solid State Communications*, 33, (1980), 1003-1004.

[140] N. Hitmi, E. Lamure-Plaino, A. Lamure, C. LaCabanne and R.A. Young, "Reorientable electric dipoles and cooperative phenomena in human tooth enamel", *Calcified Tissue International*, 38, (1986), 252 - 261.

[141] M. Ueshima, S. Nakamura and K. Yamashita, K., "Huge, Millicoulomb Charge Storage in Ceramic Hydroxyapatite by Bimodal Electric Polarization", *Advanced Materials*, 14, (2002), 591-595.

[142] B.S. Royce, 1974, "Field-induced Transport Mechanism in Hydroxyapatite", *Annals of the New York Academy of Sciences* 238, (1974), 131-138.

[143] K.A. Gross, V. Gross and C.C. Berndt, "Thermal Analysis of Amorphous Phases in Hydroxyapatite Coatings", *Journal of the American Ceramic Society*, 81, (1998), 106-112.

[144] N. Horiuchi, M. Nakamura, A. Nagai, K. Katayama, and K. Yamashita, "Proton conduction related electrical dipole and space charge polarization in hydroxyapatite", *Journal of Applied Physics*, 112, (2012), 074901.

[145] G.M. Sessler, Electrets, Laplacian, California, Vol. 1, 3rd ed., (1999).

[146] W. Liu and C.A. Randall, "Thermally Stimulated Relaxation in Fe-Doped $SrTiO_3$ Systems:I. Single Crystals", *Journal of the American Ceramic Society*, 91, (2008), 3245-3250.

[147] W. Liu and C.A. Randall, "Thermally Stimulated Relaxation in Fe-Doped SrTiO3 Systems: II. Degradation of $SrTiO_3$ Dielectrics", *Journal of the American Ceramic Society*, 91, (2008), 3251-3257.

[148] N. Wada, K. Mukougawa, N. Horiuchi, T. Hiyama, M. Nakamura, A. Nagai, T. Okura and K. Yamashita, "Fundamental electrical properties of ceramic electrets", *Materials Research Bulletin*, 48 (10), (2013), 3854-3859.

[149] N. Horiuchi, S. Nakaguki , N. Wada, K. Nozaki, M. Nakamura, A. Nagai, K. Katayama and K. Yamashita, "Polarization-induced surface charges in hydroxyapatite ceramics", *Journal of Applied Physics*, 116(1), (2014), 014902.

[150] D. Damjanovic, "Ferroelectric, dielectric and piezoelectric properties of ferroelectric thin films and ceramics", *Reports on Progress in Physics*, 61 (1998), 1267

[151] Y. Masatomo, Y. Yukihiko and F. Hirotaka, "Experimental Visualization of Chemical Bonding and Structural Disorder in Hydroxyapatite through Charge and Nuclear-Density Analysis", *The Journal of Physical Chemistry C*, 115 *(50)*, (2011), 25077-25087.

[152] S. B. Lang, S. A. M. Tofail, A.L. Kholkin, M. Wojtas, M. Gregor, A. A. Gandhi, Y.Wang, S. Bauer, M. Krause and A. Placenik, "Ferroelectric Polarization in Nanocrystalline Hydroxyapatite Thin Films on Silicon", *Scientific reports*, 3, (2013), 2215.

[153] X. Wei and M. Z. Yates, "Yttrium-Doped Hydroxyapatite Membranes with High Proton Conductivity", *Chemistry of Materials*, 24(10), (2012), 1738-1743.

[154] M. Yashima, N. Kubo, K. Omoto, H. Fujimori, K. Fujii, and K.Ohoyama, "Diffusion Path and Conduction Mechanism of Protons in Hydroxyapatite", *The Journal of Physical Chemistry C*, 118 (10), (2014), 5180-5187.

[155] N. Horiuchi, S. Nakaguki, N. Wada, K. Nozaki, M. Nakamura, A. Nagai, K. Katayama and K. Yamashita, "Polarization-induced surface charges in hydroxyapatite ceramics", *Journal of Applied Physics*, 116, (1), (2014), 014902.

[156] S. A. M. Tofail, D. Haverty, K. T. Stanton and J. B. McMonagle, "Structural Order and Dielectric Behaviour of Hydroxyapatite", *Ferroelectrics*, 319 (1), (2005), 117-123.

[157] S. A. M. Tofail, C. Baldisserri, D. Haverty, J. B. McMonagle and J. Erhart, "Pyroelectric surface charge in hydroxyapatite ceramics", *Journal of Applied Physics*, 106, (10), (2009), 106104.

[158] S. A. M. Tofail, D. Haverty, F. Cox, J. Erhart, P. Hána and V. Ryzhenko, "Direct and ultrasonic measurements of macroscopic piezoelectricity in sintered hydroxyapatite", *Journal of Applied Physics*, 105(6), (2009), 064103.

[159] A. A. Gandhi, M. Wojtas, S. B. Lang, A. L. Kholkinand and S. A.M. Tofail, "Piezoelectricity in Poled Hydroxyapatite Ceramics", *Journal of the American Ceramic Society*, 97, (2014), 2867-2872.

[160] V. S. Bystrov, "Piezoelectricity in the Ordered Monoclinic Hydroxyapatite", *Ferroelectrics*, 475 (1), (2015), 148-153.

[161] S. B. Lang, "Review of Ferroelectric hydroxyapatite and its application to biomedicine", *Phase transitions*, 89(7-8), (2016), 678-694.

[162] N. Horiuchi, Iwasaki, K. Nozaki, M. Nakamur, K. Hashimoto, A. Nagai and K. Yamashita, "A critical phenomenon of phase transition in hydroxyapatite investigated by thermally stimulated depolarization currents", *Journal of the American Ceramic Society*, 100, (2017), 501-505.

[163] N. A. Zakharov, "An analysis of the phase transitions in biocompatible $Ca_{10}(PO_4)_6(OH)_2$", *Technical Physics Letters*, 27, (12), (2001), 1035-1037.

[164] T. Ikoma, A. Yamazaki, S. Nakamura, and M. Akaro, "Preparation and Dielectric property of Sintered Monoclinic Hydroxyapatite", *Journal of Materials Science Letters*, 18 (15) (1999), 1225-1228.

[165] F. Chiatti, M. Corno, and P. Ugliengo, "Stability of the Dipolar (001) Surface of Hydroxyapatite", *The Journal of Physical Chemistry C*, 116 (10), (2012), 6108-6114.

[166] E. M. Anton, W. Jo, D. Damjanovicand and J. Rödel, "Determination of depolarization temperature of $(Bi_1/2Na_{1/2})TiO_3$-based lead-free piezoceramics", *Journal of Applied Physics*, 119(9), (2011), 094108.

[167] F. Guo, B. Yang,Bin, S. Zhang, F. Wu, D. Liu, P. Hu, Y. Sun, D. Wang and W. Cao, "Enhanced pyroelectric property in $(1-x)(Bi_{0.5}Na_{0.5})TiO_3$-$xBa(Zr_{0.055}Ti_{0.945})O_3$: Role of morphotropic phase boundary and ferroelectric-antiferroelectric phase transition", *Applied Physics Letters*, 103(18), (2013), 182906.

[168] T. N. M. Ngo, U. Adem, and T. T. M. Palstra, "The origin of thermally stimulated depolarization currents in multiferroic $CuCrO_2$", *Applied Physics Letters*, 106(15), (2015), 152904.

[169] Y. Tanaka, T. Iwasaki, M. Nakamura, A. Nagai, K. Katayama and K. Yamashita, "Polarization and microstructural effects of ceramic hydroxyapatite electrets", *Journal of Applied Physics*, 107, (2010), 014107.

[170] I. M. Kalogeras, A. V. Dova and A. Katerinopoulou, "Axially Dependent Dielectric Relaxation Response of natural Hydroxyapatite Single Crystals", *Journal of Applied Physics*, 92(1), (2002), 406-414.

[171] A. K. Dubey and K. Kakimoto, "Impedance spectroscopy and mechanical response of porous nanophase hydroxyapatite–barium titanate composite", *Materials Science and Engineering. C*, 63, (2016), 211-221.

[172] Y. Zhen and J. F. Li, "Preparation and Electrical properties of fine-scale 1-3 lead zirconictitanate epoxy composite thin films for high frequency ultrasonic transducers", *Journal of Applied Physics*, 103(8), (2008), 084119.

[173] V. Koval, M. J. Reece and A. J. Bush, "Ferroelectric/Ferroelastic behaviour and piezoelectric response of lead zirconate titanate thin films under nano identation", *Journal of Applied Physics*, 97, (2005), 074301.

[174] J. L. Jones and M. Hoffman, "Direct measurement of the domain switching contribution to the dynamic piezoelectric response in ferroelectric ceramic", *Applied Physics Letters*, 89, (2006), 092901.

[175] H. S. Kim, Y. Li and J. Kim, "Electro-mechanical behavior and direct piezoelectricity of cellulose electro-active paper", *Sensors and Actuators A: Physical*, 147 (1), (2008), 304-309.

[176] W. Jiang, W. Cao, X. Yi and H. Chen, "Elastic and Piezoelectric properties of tungsten bronze ferroelectric crystals $(Sr_{0.5}Ba_{0.3})NaNb_5O_{15}$ and $(Sr_{0.3}Ba_{0.7})_2NaNb_5O_{15}$", *Journal of Applied Physics*, 97, (2005), 094106.

[177] P. Hana, L. Burianova, S. J. Zhang, T. R. Shrout, E. Furman, V. Ryzhenko and P. Bury, "Elastic Stiffness Constants of PZN-4.5%PT Single Crystal Influenced by DC Bias Electric Field Applied at Various Directions to Prototypic Crystal Symmetry", *Ferroelectrics*, 319 (1), (2005) 145-154.

[178] IEEE Standards on Piezoelectricity (IEEE, New York, 1988).

[179] C. D. McCaig and M. Zhao M, "Physiological electrical fields modify cell behaviour", *BioEssays* 19, (1997), 819-826.

[180] R.H.W. Funk, "Endogenous electric fields as guiding cue for cell migration", *Frontiers in Physiology*, 6, (2015), 143.

[181] K. S. Kang, J. M. Hong, Y. H. Jeong, Y. J. Seol, W. J. Yong, J. W. Rhie and D. W. Cho, "Combined effect of three types of biophysical stimuli for bone regeneration", *Tissue Engineering Part A*, 20, (2014), 1767-1777.

[182] J. E. Davies, "The importance and measurement of surface charge species in cell behaviour at the biomaterial interface. In: Surface Characterisation of Biomaterials", edited by R. D. Ratner, Amsterdam: Elsevier, 1988.

[183] S. Itoh, S. Nakamura, M. Nakamura, K. Shinomiya and K. Yamashita, "Enhanced bone regeneration by electrical polarization of hydroxyapatite", *Artificial Organs*, 3, (2006), 863-839.

[184] N. C. Teng, S. Nakamura, Y. Takagi, Y. Yamashita, M. Ohgaki and K. Yamashita, "A new approach to enhancement of bone formation using electrically polarized hydroxyapatite", *Journal of Dental Research*, 80, (2001), 1925-1292.

[185] S. Nakamura, T. Kobayashi and K. Yamashita, "Numerical osteobonding evaluation of electrically polarized hydroxyapatite ceramics", *Journal of Biomedical Materials Research Part A*, 68, (2004), 90-94.

[186] M. Nakamura, S. Nakamura, Y.Sekijima, K. Niwa, T. Kobayashi and K. Yamashita, "Role of blood coagulation as intermediators of high osteoconductivity of electrically polarized hydroxyapatite", *Journal of Biomedical Materials Research Part A*, 79 (3), (2006), 627-634.

[187] A. Nagai, K. Yamashita, M. Imamura and H. Azuma, "Hydroxyapatite electret accelerates re-endothelialisation and attenuates intimal hyperplasia occurring after endothelial removal of the rabbit carotid artery", *Life Sciences*, 82 (23-24), (2008), 1162-1168.

[188] R. Okabayashi, M. Nakamura,T. Okabayashi, Y. Tanaka, A. Nagai and K. Yamashita, "Efficacy of Polarized Hydroxyapatite and Silk Fibroin Composite Dressing Gel on Epidermal Recovery From Full-Thickness Skin Wounds", *Journal of Biomedical Materials Research Part B*, 90, (2009), 641-646.

[189] H. Kim, T. Himeno, M. Kawashita, T. Kokubo and T. Nakamura, "The mechanism of biomineralization of bone-like apatite on synthetic hydroxyapatite: an in vitro assessment", *Journal of the Royal Society, Interface / the Royal Society*, 1, (2004), 17-22.

[190] Z. Schwartz and B. D. Boyan, "Underlying Mechanisms at the Bone-Biomaterial Interface", *Journal of Cellular Biochemistry*, 56, (1994), 340-347.

[191] D.A. Puleo and A. Nanci, "Understanding and controlling the bone–implant interface", *Biomaterials*, 20 (23–24), (1999) 2311-2321.

[192] J. B. Lian, "Biology of bone mineralization", *Current Opinion in Endocrinology & Diabetes*, 13 (1), (2006), 1-9.

[193] F.R. Baxter, I.G. Turner, C.R. Bowen, J.P. Gittings, J.B. Chaudhuri, "An in vitro study of electrically active hydroxyapatite-barium titanate ceramics using Saos-2 cells", *Journal of Materials Science: Materials in Medicine* 20, (2009), 1697-1708.

[194] S. Ohba, W. Wang, S. Itoh, Y. Takagi, A. Nagai and K. Yamashita, "Acceleration of new bone formation by an electrically polarized hydroxyapatite microgranule/platelet-rich plasma composite", *Acta Biomaterialia* 8, (2012), 2778–2787.

[195] M. Nakamura, A. Nagai, Y. Tanaka, Y. Sekijima and K. Yamashita, "Polarized hydroxyapatite promotes spread and motility of osteoblastic cells", *Journal of Biomedical Materials Research Part A*, 92A: (2010), 783–790.

[196] T. Kobayasi, S. Nakamura, M. Ueshima and K. Yamashita, "Mechanism of accelerated osteogenesis around polarized hydroxyapatite in the bone", *Key Engineering Materials*, 218-220, (2002), 195-198.

[197] G. Haïat, S. Naili, Q. Grimal, M. Talmant, C. Desceliers and C. Soize, "Influence of a gradient of material properties on ultrasonic wave propagation in cortical bone: Application to axial transmission", *The Journal of the Acoustical Society of America*, 125, (2009), 4043 - 4052.

[198] W Pompe, H Worch, M Epple, W Friess, M Gelinsky, P Greil, U Hempel, D Scharnweber, K Schulte, "Functionally graded materials for biomedical applications", *Materials Science and Engineering: A*, 362(1–2), (2003), 40-60.

[199] A. Sola, D. Bellucci and V. Cannillo, "Functionally graded materials for orthopedic applications – an update on design and manufacturing", *Biotechology Advances* 34 (5) (2016) 504-531.

[200] A Seidi, M Ramalingam, I Elloumi-Hannachi, S Ostrovidov and A Khademhosseini, "Gradient biomaterials for soft-to-hard interface tissue engineering", *Acta Biomaterialia*, 7(4), (2011), 1441-1451

[201] Guy M. Genin, Alistair Kent, Victor Birman, Brigitte Wopenka, Jill D. Pasteris, Pablo J. Marquez, Stavros Thomopoulos, Functional Grading of Mineral and Collagen in the Attachment of Tendon to Bone, *Biophysical Journal*, 97(4), (2009), 976-985.

[202] M. Mehrali, FS Shirazi, M. Mehrali, HSC Metselaar, NAB Kadri and NAA Osman, "Dental implants from functionally graded materials", *Journal of Biomedical Materials Research Part A*, 101A, (2013), 3046-3057.

[203] Y. C. Chen and A. Fok, "Stress distributions in human teeth modeled with a natural graded material distribution", *Dental Materials*, 30(12), (2014), e337-e348.

[204] B. Basu, Biomaterials science and tissue engineering: principles and methods. Cambridge University Press. (2017).

[205] DHA Besisa, EMM, Ewais EMM. Advances in Functionally Graded Materials and Structures, F. Ebrahimini (Ed.), London, UK: InTech. 2016, Chapter 1, pp 1-31.

[206] C. Petit, L. Montanaro and P. Palmero, "Functionally graded ceramics for biomedical application: Concept, manufacturing, and properties", *International Journal of Applied Ceramic Technology*, 15(4), (2018), 820-840.

[207] C. Zhou, C. Deng, X. Chen, X. Zhao, Y. Chen, Y. Fan and X. Zhang, "Mechanical and biological properties of the micro-/nano-grain functionally graded hydroxyapatite bioceramics for bone tissue engineering", *Journal of the Mechanical Behavior of the Biomedical Materials*, 48, (2015), 1-11.

[208] A. K. Dubey, A. EA, K. Balani and B. Basu, "Multifunctional Properties of Multistage Spark Plasma Sintered HA–$BaTiO_3$-Based Piezobiocomposites for Bone Replacement Applications", *Journal of the American Ceramic Society*, 96: (2013), 3753-3759.

[209] J. B. Park, B. J. Kelly, G. H. Kenner, A. F. von Recum, M. F. Grether, and W. W. Coffeen, "Piezoelectric Ceramic Implants: In vivo Results", *Journal of Biomedical Materials Research*, 15 [1], (1981), 103-110.

[210] J. B. Park, G. H. Kenner, S. D. Brown, and J. K. Scott, "Mechanical Property Changes of Barium Titanate (Ceramic) After in vitro and in vivo Aging," *Biomaterials, Medical Devices, and Artificial Organs*, 5 [3], (1976), 267-276.

[211] A. K. Dubey and B. Basu, "Pulsed Electrical Stimulation and Surface Charge Induced Cell Growth on Multistage Spark Plasma Sintered Hydroxyapatite-Barium Titanate Piezobiocomposite", *Journal of the American Ceramic Society*, 97, (2014), 481-489.

[212] M. Prakasam, M. Albino, E Lebraud, M Maglione, C Elissalde and A. Largeteau, "Hydroxyapatite-barium titanate piezocomposites with enhanced electrical properties", *Journal of the American Ceramic Society*, 100, (2017), 2621-2631.

[213] R. E. Jaeger, L. Egerton, "Hot pressing of potassium sodium Niobates", *Journal of the American Ceramic Society*, 45, (1962), 209-213.

[214] M. Kosec, D. Kolar, "On activated sintering and electrical properties of $NaKNbO_3$", *Materials Research Bulletin*, 10, (1975), 335-340.

[215] R. Zuo, J. Rodel, R. Chen, L. Li, "Sintering and electrical properties of lead free $Na_{.5}K_{.5}NbO_3$ piezoelectric ceramics", *Journal of the American Ceramic Society*, 89, (2006), 2010-2015.

[216] H. Wang, R. Zuo, J. Fu and Y. Liu, Sol-gel derived (Li, Ta, Sb) modified sodium potassium niobate ceramics: Processing and piezoelectric properties, *Journal of alloys and Composites* 509, (2011), 936-941.

[217] D. Khare, B. Basu and A. K. Dubey, "Electrical stimulation and piezoelectric biomaterials for bone tissue engineering applications", *Biomaterials*, 258, (2020), 120280.

[218] K. Nilsson, J. Lidman, K. Ljungstrom and C. Kjellman, "Biocompatible material for implants", *U.S. Pat.*, 6,526, 984 B1, (2003).

[219] A. K. Dubey, R. Kinoshita, K.-i. Kakimoto, "Piezoelectric sodium potassium niobate mediated improved polarization and in vitro bioactivity of hydroxyapatite", *RSC Advances*, 5(25), (2015), 19638-19646.